The regulation of SIRT2 function by cyclin-dependent kinases affects cell motility

Ruwin Pandithage,[1] Richard Lilischkis,[1] Kai Harting,[2] Alexandra Wolf,[1] Britta Jedamzik,[1] Juliane Lüscher-Firzlaff,[1] Jörg Vervoorts,[1] Edwin Lasonder,[3] Elisabeth Kremmer,[4] Bernd Knöll,[2] and Bernhard Lüscher[1]

[1]Abteilung Biochemie und Molekularbiologie, Institut für Biochemie, Universitätsklinikum, Rheinisch-Westfälische Technische Hochschule Aachen University, 52057 Aachen, Germany
[2]Interfakultäres Institut für Zellbiologie, Abt. Molekularbiologie, Universität Tübingen, 72076 Tübingen, Germany
[3]Netherland Centre for Molecular Life Sciences, Centre for Molecular and Biomolecular Informatics, 6500 HB Nijmegen, Netherlands
[4]Deutsches Forschungszentrum für Gesundheit und Umwelt, Institut für Molekulare Immunologie, 81377 München, Germany

Cyclin-dependent kinases (Cdks) fulfill key functions in many cellular processes, including cell cycle progression and cytoskeletal dynamics. A limited number of Cdk substrates have been identified with few demonstrated to be regulated by Cdk-dependent phosphorylation. We identify on protein expression arrays novel cyclin E–Cdk2 substrates, including SIRT2, a member of the Sirtuin family of NAD^+-dependent deacetylases that targets α-tubulin. We define Ser-331 as the site phosphorylated by cyclin E–Cdk2, cyclin A–Cdk2, and p35–Cdk5 both in vitro and in cells. Importantly, phosphorylation at Ser-331 inhibits the catalytic activity of SIRT2. Gain- and loss-of-function studies demonstrate that SIRT2 interfered with cell adhesion and cell migration. In postmitotic hippocampal neurons, neurite outgrowth and growth cone collapse are inhibited by SIRT2. The effects provoked by SIRT2, but not those of a nonphosphorylatable mutant, are antagonized by Cdk-dependent phosphorylation. Collectively, our findings identify a posttranslational mechanism that controls SIRT2 function, and they provide evidence for a novel regulatory circuitry involving Cdks, SIRT2, and microtubules.

Introduction

Cdks are heterodimeric enzymes with one catalytic and one regulatory subunit. Dimerization of these two subunits is essential for kinase activity. As the name suggests, some of the regulatory subunits are cyclins, including cyclin E and A, that are synthesized in a cell cycle–dependent manner. These cyclin–Cdk complexes play essential roles in controlling different phases of and the progression through the cell cycle (Nurse, 2000; Sherr and Roberts, 2004). However, other regulatory subunits have been identified that are expressed and function independently of the cell cycle (Nebreda, 2006). These include T-type cyclins and cyclin K, which associate with Cdk9 to form distinct positive transcription elongation factor b complexes and cyclin H–Cdk7, which are part of the general transcription factor complex transcription factor II H. These kinases are critical in regulating distinct steps in transcription, including the phosphorylation of components of the mediator complex and the catalytic subunit of the RNA polymerase II complex (Zurita and Merino, 2003; Marshall and Grana, 2006). Furthermore, Cdk5 associates with two regulatory subunits, p35 and 39, and these complexes are expressed primarily in postmitotic neurons as well as in other nonproliferating cells. Cdk5 has been attributed key functions during brain development, including regulation of neuronal survival, cell migration during cortical layering, neurite outgrowth, axon guidance, and synapse function (Dhavan and Tsai, 2001; Nikolic, 2004; Xie et al., 2006).

To obtain further insight into the role of Cdk-dependent regulation of cellular processes, we sought to identify novel substrates for such kinases. We chose cyclin E–Cdk2 because this kinase is an important regulator of the G1 to S-phase transition and is deregulated in a substantial fraction of human tumors (Musgrove, 2006). Indeed, elevated cyclin E expression has been linked to a poor prognosis in human breast cancer (Keyomarsi et al., 2003). Furthermore, the cyclin E–Cdk2 kinase is activated

R. Pandithage and R. Lilischkis contributed equally to this paper.

Correspondence to Bernhard Lüscher: luescher@rwth-aachen.de; or Bernd Knöll: bernd.knoell@uni-tuebingen.de

R. Pandithage's present address is Leica, 1170 Wien, Austria.

R. Lilischkis' present address is BTF Precise Microbiology, North Ryde Sydney, NSW 2113 Australia.

B. Jedamzik's present address is Max Planck Institute of Molecular Cell Biology and Genetics, 01307 Dresden, Germany.

Abbreviations used in this paper: HDAC, histone deacetylase; HDF, human diploid fibroblast; HS, horse serum; KD, knockdown; MAP, microtubule-associated protein; MEF, mouse embryonic fibroblast; ppm, parts per million; STMN2, stathmin-like 2; TAP, tandem affinity purification.

The online version of this paper contains supplemental material.

The Journal of Cell Biology, Vol. 180, No. 5, March 10, 2008 915–929
http://www.jcb.org/cgi/doi/10.1083/jcb.200707126

in response to several oncoproteins including MYC and the adenoviral E1A protein, supporting a role of this kinase in tumorigenesis (Amati et al., 1998; Luscher, 2001). Among the cyclin E–Cdk2 substrates are proteins controlling cell cycle progression, the centrosome cycle, replication, and several transcriptional regulators (Malumbres and Barbacid, 2005). Cdk2 not only associates with cyclin E but also with cyclin A, and the two complexes share several substrates. In addition, Cdk2 and 5 show similar substrate specificities (Dhavan and Tsai, 2001). In this paper we identify 26 cyclin E–Cdk2 substrates, including SIRT2, a member of the Sirtuin family that consists of seven members, SIRT1–7, in mammals (Haigis and Guarente, 2006; Michan and Sinclair, 2007). Sirtuins are class III histone deacetylases (HDAC) that require NAD^+ as a cofactor and deacetylate Lys residues. Sirtuins can be found in different compartments within the cell regulating a variety of processes, including many aspects of transcription, the lifespan of organisms, neuroprotection, tumor suppression, differentiation, and inflammation (Haigis and Guarente, 2006; Michan and Sinclair, 2007). SIRT2 is the only Sirtuin family member that is preferentially localized in the cytoplasm but, in addition, has also been implicated in nuclear functions (Dryden et al., 2003; North et al., 2003; Vaquero et al., 2006; Wilson et al., 2006; North and Verdin, 2007a).

Reversible acetylation of proteins at the ε-amino group of Lys residues has been recognized as an important posttranslational mechanism to control nuclear protein function, including histones and transcription factors (Kouzarides, 2000). In contrast, relatively little is known about acetylation/deacetylation of proteins outside the nucleus. Recent evidence, however, suggests that several cytoplasmic proteins are acetylated (Kim et al., 2006). Most notably, α-tubulin is acetylated at Lys-40 (K40), a modification that has been suggested to enhance microtubule stability (North et al., 2003). Although the acetyl transferases that modify K40 are not known, two deacetylases that physically interact, SIRT2 and HDAC6, have been implicated in removing the modification (Hubbert et al., 2002; Dryden et al., 2003; North et al., 2003; Zhang et al., 2003). It has been suggested that SIRT2 affects progression through mitosis in response to stress and that SIRT2 is regulated in mitosis by phosphorylation (Dryden et al., 2003; Inoue et al., 2007; North and Verdin, 2007b).

In this paper, we have identified in SIRT2 a single Cdk2 and 5 phosphorylation site, Ser-331 (S331), C-terminal of the catalytic domain. Phosphorylation at S331 inhibits the enzymatic activity of SIRT2. The functional analysis of SIRT2 and phosphorylation site mutants revealed that this enzyme interferes with cell adhesion in tumor cells, cell migration in fibroblasts, and neurite outgrowth and growth cone motility in neurons. Importantly, these SIRT2-mediated effects are antagonized by Cdk-dependent phosphorylation at S331. Collectively, our findings define a posttranslational mechanism that regulates SIRT2 function both in vitro and in cells.

Results

Identification of novel cyclin–Cdk substrates

To identify novel cyclin E–Cdk2 substrates, high-density protein arrays on polyvinylidine difluoride filters were phosphorylated with recombinant baculoviral cyclin E–Cdk2 and γ-[^{32}P]ATP (Fig. 1 A). The clones corresponding to 96 prominent substrates were sequenced and revealed 42 clones that expressed the ORF in frame with the N-terminal tag. These represented 26 different proteins, some known Cdk substrates, with potential phosphorylation sites and cyclin binding motifs (Table I). These substrates, bacterially expressed HIS or GST fusion proteins, were verified in in vitro kinase assays using different cyclin–Cdk complexes. Similar amounts of kinase activities were used as assessed with Rb and histone H1 as substrates (Fig. 1 B). All proteins identified in the screen, except one (RPL14), were phosphorylated by cyclin E–Cdk2, demonstrating that these are true positive in vitro substrates (Table I and Fig. S1, available at http://www.jcb.org/cgi/content/full/jcb.200707126/DC1). As expected, many of the cyclin E–Cdk2 substrates were also phosphorylated by cyclin A–Cdk2 and, strikingly, by cyclin D3–Cdk4 but not by cyclin B–Cdk1 or cyclin D1–Cdk4 (Table I and Fig. S1). We observed cyclin D3 phosphorylation of the purified cyclin D3–Cdk4 complex (Fig. 1, B and C; and Fig. S1), although D-type cyclins have not been described to be autophosphorylated. However, because this phosphorylation was completely repressed by $p16^{INK4A}$, an inhibitor of D-type kinase complexes, it is most likely mediated by Cdk4 (Fig. S1 A). In this paper, we chose to further investigate SIRT2, a member of the Sirtuin family of NAD^+-dependent deacetylases.

Phosphorylation of SIRT2 by Cdks

The findings from the screen were verified by phosphorylating a GST-SIRT2 fusion protein by the different purified kinase complexes (Fig. 1 and Fig. S2, available at http://www.jcb.org/cgi/content/full/jcb.200707126/DC1). SIRT2 was a substrate for cyclin E–Cdk2 and, to a lesser extent, cyclin A–Cdk2 (Fig. 1 C). In addition SIRT2 was weakly phosphorylated by cyclin D3–Cdk4 and cyclin B–Cdk1 but not by cyclin D1–Cdk4 (Fig. 1 C). Inspection of the human SIRT2 protein sequence revealed a single consensus sequence for Cdks, S_{331}PKK, which is C terminal of the catalytic domain (Fig. 1 D) and is conserved in mouse SIRT2. Similar phosphorylation sites at comparable positions relative to the catalytic domains are found in the SIRT family members SIRT1, 6, and 7 (Fig. 1 D) and are phosphorylated by Cdk2 in vitro (not depicted). To address whether S331 is phosphorylated by Cdk2, GST-SIRT2 fusion proteins with S331 mutated to Ala, Asp, or Glu were phosphorylated with recombinant cyclin E–Cdk2 or cyclin A–Cdk2. Mutation of S331 abolished Cdk2-dependent phosphorylation (Fig. 1 E; and Fig. S2, A–C). The reactions were specific because roscovitine, a Cdk inhibitor, abolished SIRT2 phosphorylation (Fig. S2, A and C). In addition, S331 phosphorylation by cyclin E–Cdk2 in vitro was confirmed by mass spectrometry analysis (Fig. S2 D).

SIRT2 is highly expressed in the nervous system (Fig. S3, available at http://www.jcb.org/cgi/content/full/jcb.200707126/DC1), which is in agreement with previous reports (Li et al., 2007; Southwood et al., 2007). Similarly, in the nervous system, Cdk5 is strongly expressed in postmitotic neuronal cells, unlike Cdk2, which is down-regulated when neurons exit the cell cycle and differentiate (Freeman et al., 1994). Therefore, we tested whether a p35–Cdk5 complex could phosphorylate SIRT2.

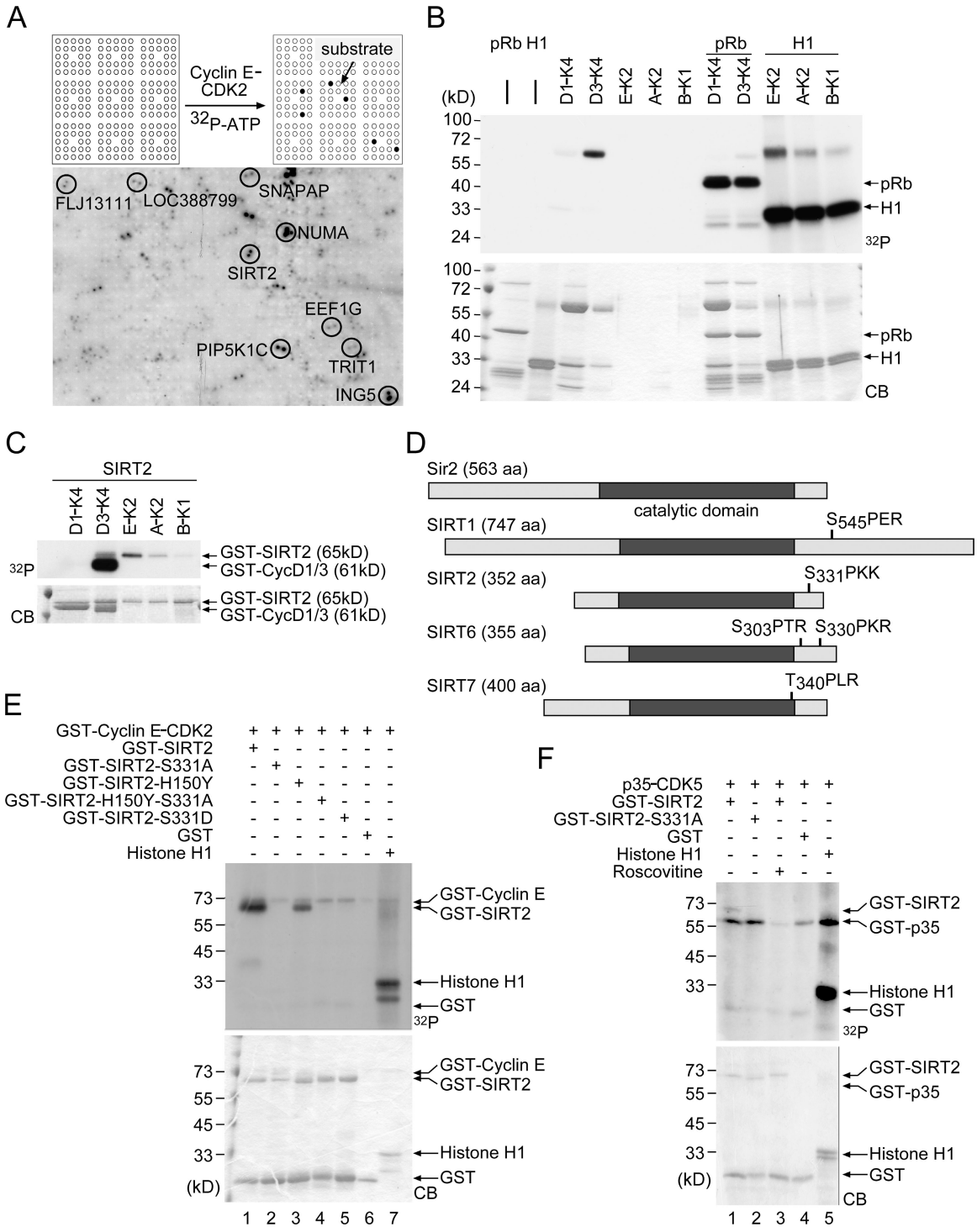

Figure 1. **Identification of SIRT2 as a Cdk substrate.** (A) High-density protein arrays (two filters with 37,830 clones preselected for high protein expression by virtue of N-terminal 6xHIS tags [Bussow et al., 1998]) were incubated with recombinant human cyclin E–Cdk2 and γ-[^{32}P]ATP, washed, and exposed to x-ray film. Potential substrates appear as double spots, as indicated by circles. A portion of one filter is displayed. (B) cyclin–Cdk complexes were incubated with or without their respective substrates (Cdk4 complexes with GST-pRb$^{773\text{-}928}$ and Cdk2 and 1 complexes with histone H1) and γ-[^{32}P]ATP. Proteins were resolved by 7–17% SDS-PAGE and visualized by autoradiography (^{32}P, top) or Coomassie blue staining (CB, bottom). Kinase complexes are abbreviated (e.g., D1–K4 for cyclin D1–Cdk4). (C) Bacterially expressed GST-SIRT2 full-length fusion protein was phosphorylated with the indicated kinases as described in B. (D) Schematic comparison of *Saccharomyces cerevisiae* Sir2 with human SIRT1, 2, 6, and 7. The catalytic domains and the potential Cdk phosphorylation sites are indicated. (E) Bacterially expressed GST-SIRT2 fusion proteins, as indicated, were phosphorylated with 25 fcatal cyclin E–Cdk2. GST and histone H1 served as controls. Protein analysis was performed as in B. (F) The experiment was performed as in E with 3 fcatal of recombinant p35–Cdk5. For a control, 25 μM roscovitine was added to inhibit Cdk5 activity.

Table I. **In vitro phosphorylation of potential cyclin E–Cdk2 substrates by different cyclin–Cdk complexes**

Potential cyclin E–Cdk2 substrate			Phosphorylation sites and cyclin binding motifs in the RZPD clone			Phosphorylation of the RZPD clone by kinases[a]				
Gene	ORF of RZPD clone	Name/biological process	min: S/TP	cons: S/TPXK/R	RXL	D1–K4	D3–K4	E–K2	A–K2	B–K1
NUMA1[b]	245 aa C-term	Nuclear mitotic apparatus protein 1/ spindle apparatus organization	7	1	0	−	±	+	+	−
LOC201191	231 aa C-term	Hypothetical protein LOC201191/unknown	6	1	2	−	±	+	+	−
PIP5K1C	200 aa C-term	Phosphatidylinositol-4-phosphate 5 kinase, type I γ/phosphatidylinositol signaling	7	2	1	±	+	+	+	±
CCNL2	136 aa C-term	cyclin L2 / RNA processing	7	3	2	−	−	±	+	±
RASL11B	118 aa C-term	RAS-like, family 11, member B/signaling?	2	1	0	−	+	+	+	−
SIRT2	full-length[c]	Sirtuin (silent mating type information regulation 2 homologue) 2 (*S. cerevisiae*)/ NAD^+-dependent histone/protein deacetylase	3	1	1	−	−	+	+	±
FLJ13111	full-length	Hypothetical protein FLJ13111/unknown	4	2	4	−	±	+	+	±
SUPT5H[b]	120 aa C-term	Suppressor of Ty 5 homologue (*S. cerevisiae*)/transcription	1	1	1	−	−	±	−	−
STMN2[b]	full-length	Stathmin-like 2/microtubule destabilization in neuronal growth	2	1	1	−	+	+	+	−
LOC146909	114 aa C-term	Hypothetical protein LOC146909/unknown	1	0	1	−	+	+	+	−
EEF1G	211 aa C-term	Eukaryotic translation elongation factor 1γ/translation	2	1	1	−	±	+	+	±
TRIT1	99 aa C-term	tRNA isopentenyltransferase 1/ RNA modification	3	1	1	−	+	+	+	±
LOC388799	89 aa C-term	Hypothetical protein LOC388799/unknown	2	1	0	−	±	+	+	±
STUB1	full-length	STIP1 homology and U-box–containing protein 1/protein turnover	4	1	3	−	+	+	+	±
SRRM2	98 aa central	Serine/arginine repetitive matrix 2/ RNA processing	3	0	0	−	−	+	+	+
TALDO1	full-length	Transaldolase 1/metabolism	3	1	6	−	+	+	+	−
SFRS1	243 aa C-term	Splicing factor, arginine/serine-rich 1 (splicing factor 2, alternate splicing factor)/RNA processing	4	1	1	−	+	+	+	−
SNAPAP	full-length	SNAP-associated protein/exocytosis of synaptic vesicles	2	1	2		+	±	+	
LOC339287	90 aa central	Hypothetical protein LOC339287/unknown	5	4	1	+	+	+	+	+
FLJ12949	248 aa C-term	Hypothetical protein FLJ12949/unknown	4	1	3	−	+	+	−	−
MAP2	376 aa C-term	MAP2/microtubule assembly in neurogenesis	16	3	1	−	+	+	+	−
RPL14	211 aa C-term	Ribosomal protein L14/translation	1	1	1	−	±	−	−	−
FNBP3	245 aa C-term	Formin binding protein 3/splicing?	2	1	1	−	±	±	±	−
PRC1[d]	full-length	Protein regulating cytokinesis 1/ cytokinesis	5	2	2	−	+	+	+	±
FLJ13305	162 aa central	Hypothetical protein FLJ13305/unknown	4	0	3	−	+	+	±	−
ING5	full-length[c]	Inhibitor of growth family, member 5/ p53 pathway, replication	2	1	3	−	−	+	+	−

[a]The kinases used are abbreviated (e.g., D1–K4 for cyclin D1–Cdk4). The substrates are phosphorylated strongly (+), weakly (±), or not at all (−) by the respective kinase.
[b]Previously reported Cdk substrate (Stachora et al., 1997; Gavet et al., 1998; Sun and Schatten, 2006).
[c]For ING5 and SIRT2, GST-tagged full-length proteins were used in the kinase assays.
[d]Previously reported cyclin E–Cdk2 substrate (Jiang et al., 1998).

Similar to cyclin E–Cdk2 and cyclin A–Cdk2 complexes, p35–Cdk5 was capable of phosphorylating SIRT2 at S331 (Fig. 1 F), suggesting that this site can be phosphorylated both in cycling and differentiated cells.

To corroborate the in vitro kinase assays, we analyzed the phosphorylation of SIRT2 in cells (Fig. 2). HA-tagged SIRT2 or SIRT2-S331A was expressed in HeLa cells and labeled with [^{32}P]orthophosphate. Although SIRT2 was phosphorylated, the S331A mutant was only poorly labeled (Fig. 2 A). Moreover, coexpression of the Cdk2 inhibitor p27^{KIP1} abolished SIRT2 phosphorylation (Fig. 2 A). We also generated HEK293 cells stably expressing a tagged version of SIRT2 (N–tandem affinity purification [TAP]–SIRT2; Fig. S4, available at http://www.jcb.org/cgi/content/full/jcb.200707126/DC1). The analysis of TAP-SIRT2 isolated from exponentially growing cells by mass spectrometry confirmed SIRT2 phosphorylation at S331 (Fig. 2 B). In support of this, a peptide that contains S331 was identified as phosphopeptide in a global screen (Olsen et al., 2006). In addition, SIRT2 phosphorylation was high in cells blocked in S-phase and in prometaphase by hydroxyurea and nocodazole, respectively, but low in cells blocked in metaphase by colcemide when analyzed by [^{32}P]orthophosphate labeling (Fig. 2 C) and mass spectrometry (not depicted). This correlates with active cyclin E–Cdk2 and cyclin A–Cdk2 kinase complexes, implicating these kinases in SIRT2 phosphorylation. In summary, these findings define S331 as the major cell cycle–regulated Cdk-dependent phosphorylation site of SIRT2.

To expand on the observations described in the previous paragraph, we addressed whether endogenous SIRT2 is phosphorylated at Ser-331. We generated mAbs against a human SIRT2 Ser-331 phosphorylated peptide. The antibodies were screened on HA-SIRT2 and HA-SIRT2-S331A. Although mAb 7G5 recognized both proteins, mAb 6B5^{P} detected only HA-SIRT2 (Fig. S2 E). In support of this, the epitope was lost when overexpressed HA-SIRT2 was phosphatase treated, indicating that mAb 6B5^{P} is phosphospecific (Fig. S2 F). Importantly the 6B5^{P} epitope was generated when bacterially expressed GST-SIRT2 was phosphorylated by cyclin E–Cdk2 (Fig. 2 D). We then addressed whether endogenous SIRT2 was phosphorylated at Ser-331. Because in multiple cell lines analyzed SIRT2 levels were low and did not allow direct analysis by Western blotting, we examined Ser-331 phosphorylation upon immunoprecipitation of endogenous SIRT2. HEK293 cells were arrested in S-phase using hydroxyurea to enhance cyclin E–Cdk2–dependent phosphorylation and treated the cells for the last 2 h with roscovitine, a Cdk2 inhibitor. In HEK293 cells, the two described SIRT2 isoforms, a consequence of alternative splicing (North and Verdin, 2007b), were detected with the phosphospecific mAb 6B5^{P} (Fig. 2 E). Roscovitine treatment reduced SIRT2 phosphorylation by at least 60% and the 6B5^{P} epitope was sensitive to phosphatase treatment (Fig. 2 E). Reduced phosphorylation correlated with the appearance of SIRT2 protein species with slightly increased mobility (Fig. 2 E, double bands). To address cell cycle regulation, serum-starved primary human diploid fibroblasts (HDFs) were stimulated with serum and entered S-phase by 18 h as monitored by BrdU incorporation (unpublished data). Although overall levels of SIRT2 (only the larger isoform was detectable in HDFs) did not change, phosphorylation increased (Fig. 2 F). This observation is in agreement with cyclin E–Cdk2 functioning as a SIRT2 kinase (Fig. 1 E), the sensitivity of SIRT2 phosphorylation to the cyclin E–Cdk2 inhibitor p27 (Fig. 2 A), the cell cycle analysis (Fig. 2 C), and the sensitivity of SIRT2 phosphorylation to roscovitine (Fig. 2 E).

To further strengthen the functional interaction of SIRT2 with Cdk complexes, we analyzed whether these proteins interacted physically. Coimmunoprecipitation experiments revealed that SIRT2 and cyclin E–Cdk2 interacted when coexpressed in HEK293 cells (Fig. 2 G) and cyclin E bound to SIRT2 in in vitro pulldown experiments (not depicted). Furthermore, TAP-SIRT2, TAP-SIRT2-S331A, and TAP-SIRT2-H150Y, but not TAP-SIRT2-S331D, interacted with endogenous cyclin E in HEK293 cells stably expressing the SIRT2 proteins (Fig. S2 G). Similarly, p35 and Cdk5 were coimmunoprecipitated with SIRT2 upon overexpression in HEK293 cells (Fig. 2 H). Interaction of endogenous p35–Cdk5 and SIRT2 was demonstrated by coimmunoprecipitation from P14 mouse brain extracts (hippocampus and cortex; Fig. 2, I and J). Furthermore, in addition to previous reports showing SIRT2 expression mainly in oligodendroglial cells (Li et al., 2007; Southwood et al., 2007), primary hippocampal neurons expressed SIRT2 throughout the cell body in the neurites and growth cones (Fig. S5, available at http://www.jcb.org/cgi/content/full/jcb.200707126/DC1). Moreover, SIRT2 colocalized with p35, the regulatory subunit of Cdk5 (Fig. S5, A–D), and SIRT2 expression overlapped with acetylated α-tubulin in neuronal growth cones (Fig. S5, E–G). Thus p35, which has recently been shown to directly bind to microtubules (Hou et al., 2007), colocalizes with SIRT2 and α-tubulin. In summary, these findings support our phosphorylation analysis and the notion that Cdk complexes, SIRT2, and α-tubulin interact functionally.

Phosphorylation at S331 inhibits the catalytic activity of SIRT2

Next we assessed the functional relevance of S331 phosphorylation. No difference in the subcellular distribution of SIRT2 and SIRT2-S331 mutants or the stability of these proteins could be observed (unpublished data). Importantly, however, S331 phosphorylation affected the catalytic activity of SIRT2. GST-SIRT2 showed robust NAD^{+}-dependent deacetylase activity toward core histones, which was blocked by nicotinamide (Fig. 3 A). GST-SIRT2-S331A had comparable deacetylase activity when adjusted to protein concentrations (Fig. 3, A and B). In contrast, GST-SIRT2-S331D, a mutation that may mimic phosphorylation at S331, showed reduced activity (Fig. 3, A and B). All mutants with the active center His-150 (H150) changed to Tyr were catalytically inactive as reported previously (Frye, 1999). These findings suggested that phosphorylation at S331 inhibits the enzymatic activity of SIRT2. Indeed, when GST-SIRT2 was incubated in the presence of cyclin E–Cdk2 or cyclin A–Cdk2, the catalytic activity of SIRT2 was repressed (Fig. 3, C and D). These kinase-dependent effects required S331 because GST-SIRT2-S331A was not inhibited. Moreover, roscovitine reversed the repressive effect (Fig. 3 C). It is noteworthy that although p35–Cdk5 phosphorylated S331 (Fig. 1 F), the

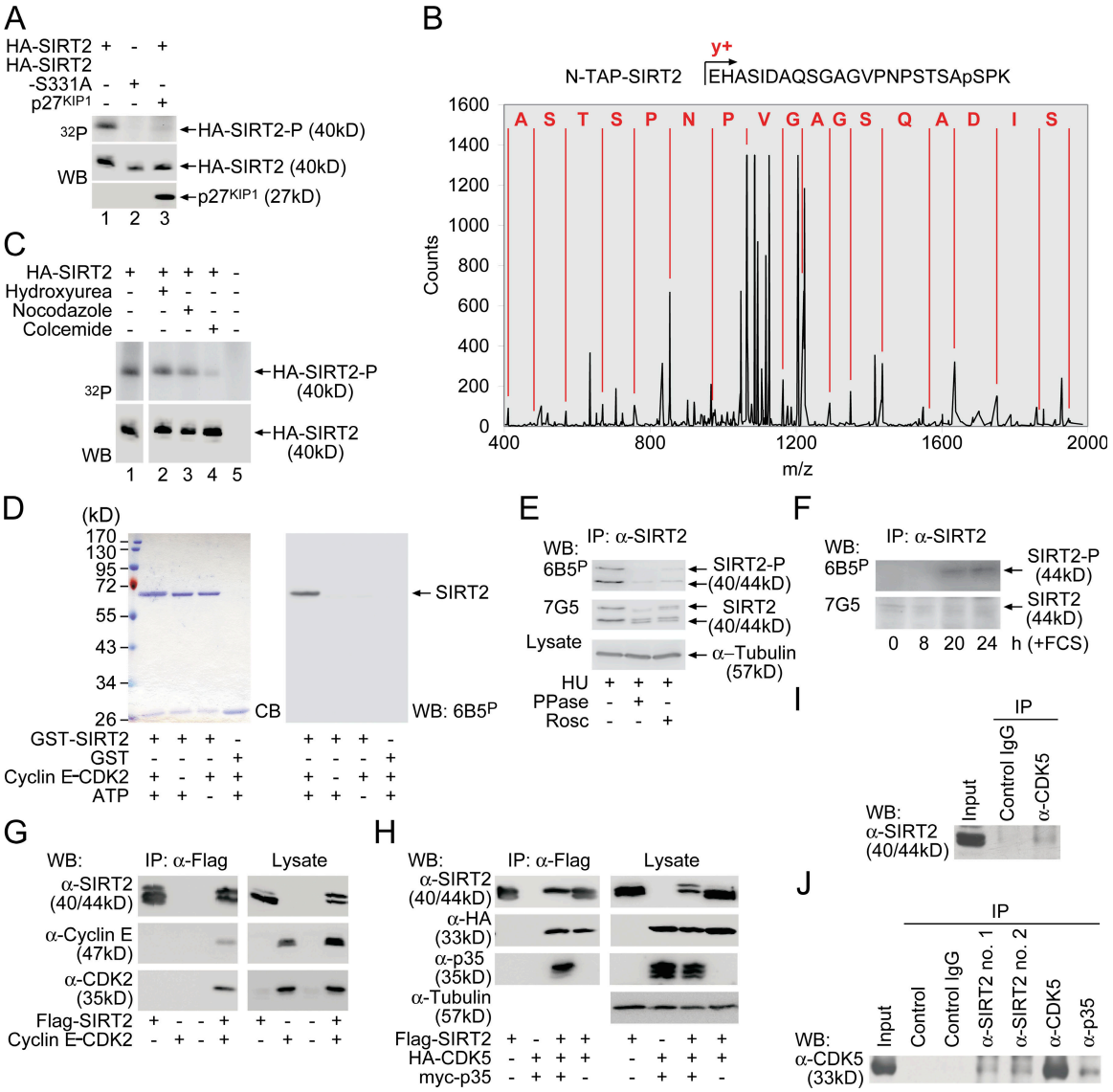

Figure 2. **SIRT2 is phosphorylated at serine 331 in cells and interacts with Cdk complexes.** (A) HEK293 cells were transiently transfected with plasmids encoding 10 µg HA-SIRT2, 10 µg HA-SIRT2-S331A, and 5 µg p27, as indicated, and metabolically labeled with [^{32}P]orthophosphate. SIRT2 was then immunoprecipitated via its HA-tag. The top shows an autoradiography, the bottom shows Western blots for HA-SIRT2 (mAb 3F10) and p27^{KIP1} (C-19). (B) N-TAP-SIRT2 was purified from HEK293 cells. The fragmentation spectrum of parent ion m/z 1144.5163, 2 + (mass accuracy, 2.8 ppm) is shown. Mascot searches against the Uniprot database identified that this peptide unambiguously phosphorylated at position Ser-331 with a Mascot ion score of 68 (Expectance value, 1.9*E-4). The phosphopeptide was sequenced eight times from two unique overlapping peptide sequences because of the presence of miscleaved tryptic sites. The y-ion fragmentation ladder starting from the C terminus is shown in red. The phosphorylation site was mapped by the detection of the y^+_3 fragment ion in the linear ion trap at m/z 411.3, which corresponds to the sequence pSPK. (C) HEK293 cells were transiently transfected with a plasmid encoding 10 µg HA-SIRT2 and treated with 200 µM hydroxyurea, 400 ng/ml nocodazole, or 200 ng/ml colcemide for 20 h and then metabolically labeled with [^{32}P]orthophosphate. The SIRT2 analysis was performed as described in A. White lines indicate that intervening lanes have been spliced out. (D) Bacterially expressed and purified GST-SIRT2 or GST was phosphorylated by recombinant cyclin E–Cdk2 in the presence or absence of ATP as indicated. Half of the reactions were analyzed by Coomassie blue (CB) staining, the other half were subjected to Western blot analysis using the mAb 6B5^P that is specific for Ser-331 phosphorylated SIRT2. (E) HEK293 cells were treated as indicated with hydroxyurea (HU) for 16 h and with roscovitine (Rosc) for the last 2 h. SIRT2 was immunoprecipitated using the polyclonal serum 748 from RIPA lysates of 6 × 10^6 cells. The immunoprecipitated proteins were phosphatase or mock treated and the proteins were analyzed by Western blotting with the indicated mAbs. Equal aliquots of the lysates were taken before immunoprecipitation and α-tubulin expression was determined. (F) Primary HDFs were serum starved and then treated with 10% serum for the indicated times. Parallel samples were analyzed for BrdU incorporation, indicating that the cells started to enter S-phase 18 h after serum addition. SIRT2 was immunoprecipitated from lysates of roughly 4 × 10^6 cells per sample and detected with the indicated mAbs. (G) HEK293 cells were cotransfected with Flag-SIRT2, cyclin E, and Cdk2 construct. Their expression was visualized in total cell lysates by Western blotting (right). Flag-SIRT2 was immunoprecipitated and the association of coexpressed cyclin E and Cdk2 analyzed by Western blotting (left). (H) The experimental setup and analysis was as in D. Constructs expressing Flag-SIRT2, HA-Cdk5, and myc-p35 were used. (I) Low-stringency lysates of P14 mouse brain were generated and Cdk5 was immunoprecipitated. Coimmunoprecipitated SIRT2 was visualized by Western blotting. (J) The experiment was performed as in F. SIRT2 was immunoprecipitated with two different polyclonal antisera (T749 and T809). For a control, p35 and Cdk5 were immunoprecipitated. Cdk5 coimmunoprecipitated with SIRT2 was monitored by Western blotting.

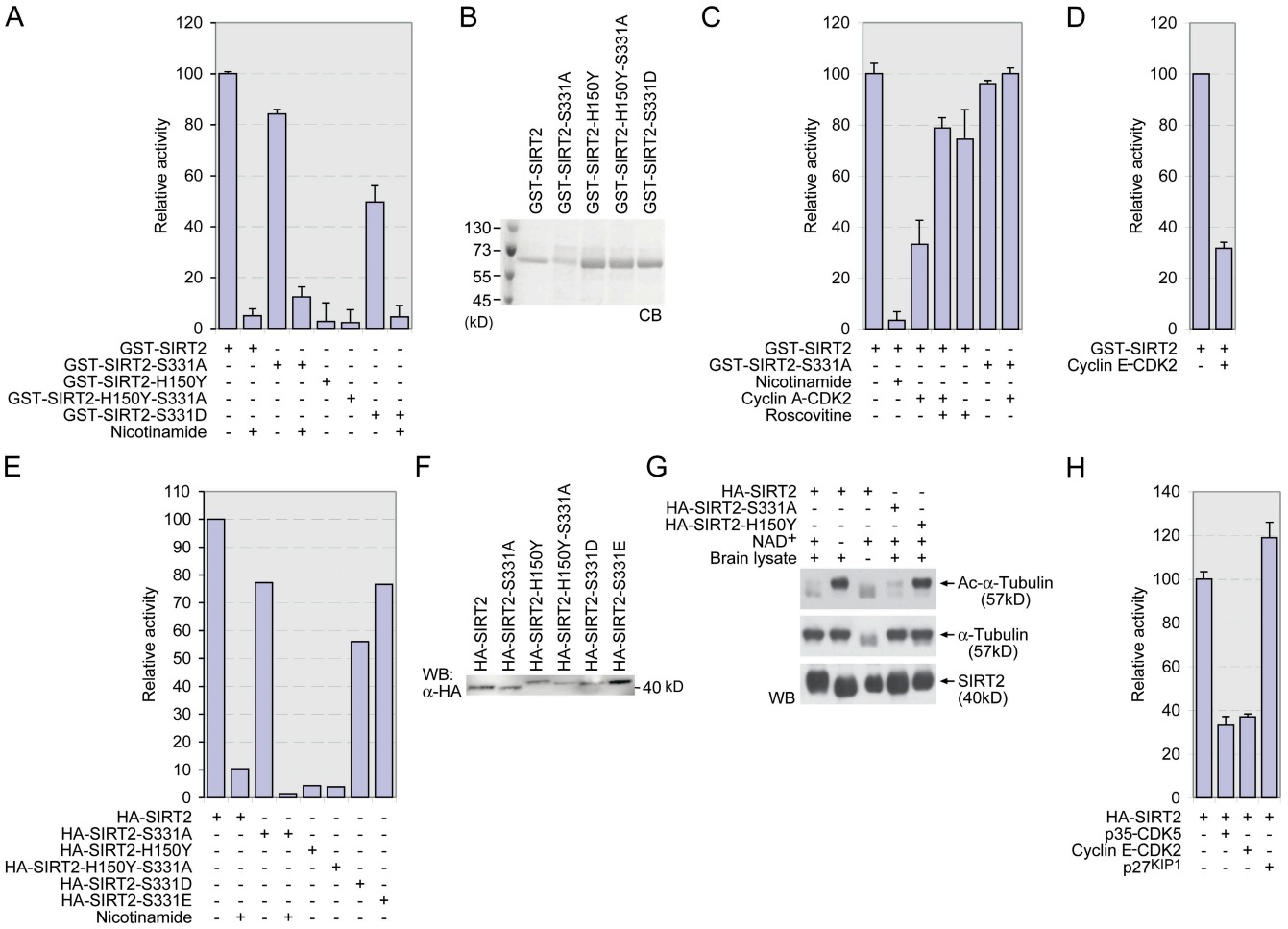

Figure 3. **Phosphorylation at serine 331 inhibits the catalytic activity of SIRT2.** (A) The indicated bacterially expressed and purified GST-SIRT2 fusion proteins were used in HDAC assays. The release of radioactivity from ^{3}H-acetylated core histones was determined. The activity of GST-SIRT2 was set as 100%. Nicotinamide was used at 10 mM. Mean values and SD of three experiments are shown. (B) Coomassie blue staining of GST-SIRT2 fusion proteins used in A. (C and D) HDAC assays were performed as in A. Before this, the GST-SIRT2 proteins were phosphorylated with recombinant cyclin A–Cdk2 and cyclin E–Cdk2 complexes. Nicotinamide and roscovitine were used at 10 mM and 25 μM, respectively. Mean values and SD of three experiments are shown. (E) HEK293 cells were transiently transfected with 10 μg of plasmids encoding the indicated SIRT2 proteins. The HA-tagged proteins were immunoprecipitated and the associated HDAC activity was determined as described in A. The assays were performed in the presence of 20 μM trichostatin A to inhibit class I or II HDACs that were potentially associated with the immunoprecipitates. Nicotinamide was used at 10 mM. A typical experiment is shown. (F) Aliquots of the immunoprecipitates (10%) used in E were analyzed by Western blotting using mAb 3F10, which is specific for the HA-tag. (G) SIRT2 and SIRT2 mutants were expressed in HEK293 cells, immunoprecipitated, and assayed for α-tubulin deacetylase activity using brain extracts as a source for substrate. Acetylation of α-tubulin was determined by Western blotting. (H) The experiments were performed as described in E. The relative activities were standardized to SIRT2 protein expression. Mean values and SD of an experiment performed in triplicate are shown.

poor catalytic activity and the instability of this commercially available complex did not allow us to directly test its in vitro effects on SIRT2 catalytic activity. However, because p35–Cdk5 also phosphorylates S331, it is highly likely that the deacetylase activity of SIRT2 would be inhibited.

Finally, we addressed whether SIRT2 expressed in mammalian cells was catalytically active. HA-SIRT2 and mutants were expressed in HEK293 cells, immunoprecipitated, and assayed for HDAC activity (Fig. 3, E and F). As for the bacterially expressed proteins, SIRT2 had comparable activities to SIRT2-S331A, whereas the phospho-mimicking mutants were less active when compared with input. In addition, nicotinamide inhibited the catalytic activity and SIRT2-H150Y was inactive (Fig. 3, E and F). Furthermore, SIRT2 and SIRT2-S331A, but not SIRT2-H150Y, deacetylated α-tubulin in brain extracts in a NAD^{+}-dependent manner (Fig. 3 G). Finally, we coexpressed SIRT2 with cyclin E–Cdk2 or p35–Cdk5 and measured HDAC activity of immunoprecipitated SIRT2. Both kinases inhibited, whereas p27^{KIP1} slightly stimulated, the catalytic activity of SIRT2 (Fig. 3 H). Collectively, our data demonstrate that phosphorylation at S331 represses the enzymatic activity of SIRT2.

SIRT2 regulates cell adhesion and cell migration

It had been suggested that SIRT2 affects passage through mitosis, possibly as a consequence of altered α-tubulin acetylation (Dryden et al., 2003; North et al., 2003). Therefore, we tested whether SIRT2 and mutants altered the cell cycle in HeLa and HEK293 cells. No systematic effects on cell cycle distribution and proliferation could be measured (Fig. S4). However, we

noticed cell detachment upon induction of SIRT2-S331A in HEK293 cells and analyzed this further. SIRT2 and SIRT2-S331A resulted in a 2.5- and 4-fold increase, respectively, of detached cells (Fig. 4, A and B). Importantly, the catalytically inactive mutant SIRT2-H150Y and the phospho-mimicking mutant SIRT2-S331D with reduced catalytic activity had no effect (Fig. 4 B). SIRT2-mediated inhibition of cell adhesion coincided with a reduced α-tubulin acetylation (Fig. 4 C). Conversely, knockdown (KD) of SIRT2 using a siRNA that targets both human and mouse *SIRT2* increased substratum adhesion of transfected cells and resulted in an increase of α-tubulin acetylation (Fig. 4, D and E). Cyclin E–Cdk2 or p35–Cdk5 efficiently inhibited SIRT2-induced cell detachment (Fig. 4 D) but had no effect on SIRT2-S331A (Fig. 4 F). To test whether SIRT2 also affected cell adhesion of primary cells, we expressed SIRT2 and mutants in mouse embryonic fibroblasts (MEFs). Similar to the observation in HEK293 cells, SIRT2 and SIRT2-S331A inhibited attachment of MEF cells to laminin-coated coverslips in comparison with the catalytically inactive SIRT2-H150Y (Fig. 4 G). In addition to cell adhesion, SIRT2 function was explored in migration of MEF cells (Fig. 4 H). A mechanical scratch was applied to MEF monolayers transiently expressing SIRT2 or SIRT2 mutants and reinvasion of the cleared area by cells was monitored. In line with the results obtained in cell adhesion (Fig. 4, A–F), SIRT2 slightly, and SIRT2-S331A significantly, blocked migration of MEFs (Fig. 4 H). These findings suggest that altering the SIRT2 activity in cells affects the interaction of cells with the substratum, possibly by altering the stability of microtubules because of differential acetylation.

SIRT2 overexpression inhibits neurite outgrowth

The intimate link between p35–Cdk5 and SIRT2, as shown by the ability of Cdk5 to phosphorylate SIRT2 (Fig. 1 F), which is shown by coimmunoprecipitation studies (Fig. 2, I and J) and deacetylation assays (Fig. 3 H), suggests that SIRT2 functions as a novel downstream effector of Cdk5. Microtubules possess pivotal functions in regulating multiple aspects of neuronal motility, including migration, neurite outgrowth, and growth cone turning (Dent and Gertler, 2003; Gordon-Weeks, 2004). Cdk5 has been implicated in all these processes (Dhavan and Tsai, 2001; Nikolic, 2004). Therefore, we first assessed the role of SIRT2 in neurite formation and protrusion (Fig. 5). Primary mouse hippocampal neurons were coelectroporated with SIRT2 and GFP-expressing plasmids and cultured for 2 d on laminin to promote neurite outgrowth. The cells were then stained for acetylated α-tubulin and the neurite length of GFP-positive cells was determined (Fig. 5). SIRT2 and, more profoundly, SIRT2-S331A reduced neurite length, whereas SIRT2-H150Y, SIRT2-H150Y-S331A, SIRT2-S331E, and SIRT2-S331D had no effect (Fig. 5, A and B; and not depicted). Of note, quantification of the neurite length (Fig. 5 B) underestimated the consequence of SIRT2-S331A expression because in more than half of the cells, neurite formation was completely abolished, resulting in a rounded-up phenotype (Fig. 5, A and C). This was not observed for SIRT2, which can be phosphorylated and thereby inhibited. Acetylation of α-tubulin was reduced by SIRT2-S331A and, to a lesser extent, by SIRT2 (Fig. 5 D; and not depicted). In agreement with SIRT2 being a novel Cdk5 effector, SIRT2-mediated, but not SIRT2-S331A-mediated, neurite outgrowth inhibition was rescued at least partially by p35–Cdk5 (Fig. 5 E).

The overexpression findings were complemented by KD of SIRT2, which resulted in a significant increase of neurite length (Fig. 5, F and G). Notably, the number of neurons with very long neurites (>150 μm) was increased almost threefold in SIRT2 KD cells (Fig. 5 G). Finally, we also observed an increase in total neurite number (on average 25%) per neuron upon SIRT2 KD (unpublished data), further stressing SIRT2's inhibitory role in neurite outgrowth. To address potential off-target effects, we used a second mouse-specific *SIRT2* siRNA that also increased neurite length (unpublished data), whereas a human-specific *SIRT2* siRNA was indistinguishable from siLUC. In summary, these findings demonstrate a decisive role of SIRT2 in neurite outgrowth of primary neurons, which is in agreement with its role in oligodendroglial arborization (Li et al., 2007).

SIRT2 impairs cytoskeletal growth cone dynamics stimulated by repulsive axon guidance cues

A well-established paradigm to study axon guidance in tissue culture is the so-called growth cone collapse assay. Members of the ephrin-A family trigger growth cone repulsion through stimulating EphA receptor tyrosine kinases, thereby preventing growth cones from turning into aberrant target areas of the brain (Knoll and Drescher, 2002; Pasquale, 2005). Cdk5 is a key mediator of EphA receptor-mediated repulsion (Cheng et al., 2003; Fu et al., 2007). Consequently, we explored the role of SIRT2 in growth cone collapse. Hippocampal neurons revealed typical well-elaborated growth cones with finger-like filopodial and veil-like lamellipodial structures in response to Fc control proteins (Fig. 6 A). In contrast, ephrin-A5-Fc induced a complete breakdown of the growth cone F-actin cytoskeleton within 30 min, leaving the neurites with a retracted neurite shaft (Fig. 6, A and B; Knoll et al., 2006). Importantly the growth cones of neurons expressing SIRT2 or SIRT2-S331A, but not SIRT2-S331 A-H150Y, SIRT2-S331E, or SIRT2-S331D, were resistant to ephrin-A5-Fc–induced collapse (Fig. 6, A–C; and not depicted). Thus, ephrin-A5-Fc collapsed 60–70% of the growth cones, an effect that was reduced to 30–40% by SIRT2 and SIRT2-S331A (Fig. 6 B). In summary, the reduction in growth cone collapse by SIRT2 and SIRT2-S331A was ∼50 and 75%, respectively (Fig. 6 C). Similar to the reduced α-tubulin acetylation in the entire neuron (Fig. 5 D), we determined a reduction of acetylated α-tubulin as compared with the control by 40 and 25% in response to SIRT2-S331A and SIRT2, respectively, in growth cones (not depicted).

F-actin staining was reduced 2.5-fold upon ephrin-A5-Fc treatment (Fig. 6 D). This could not be further enhanced by coexpressing p35–Cdk5, although the expression of this kinase complex slightly reduced F-actin staining in the absence of ephrin-A5-Fc. Importantly, and in accordance with the morphological assessment of growth cone collapse (Fig. 6, A–C), the expression of SIRT2 and SIRT2-S331A blocked the ephrin-A5-Fc–induced growth cone collapse as revealed by F-actin staining.

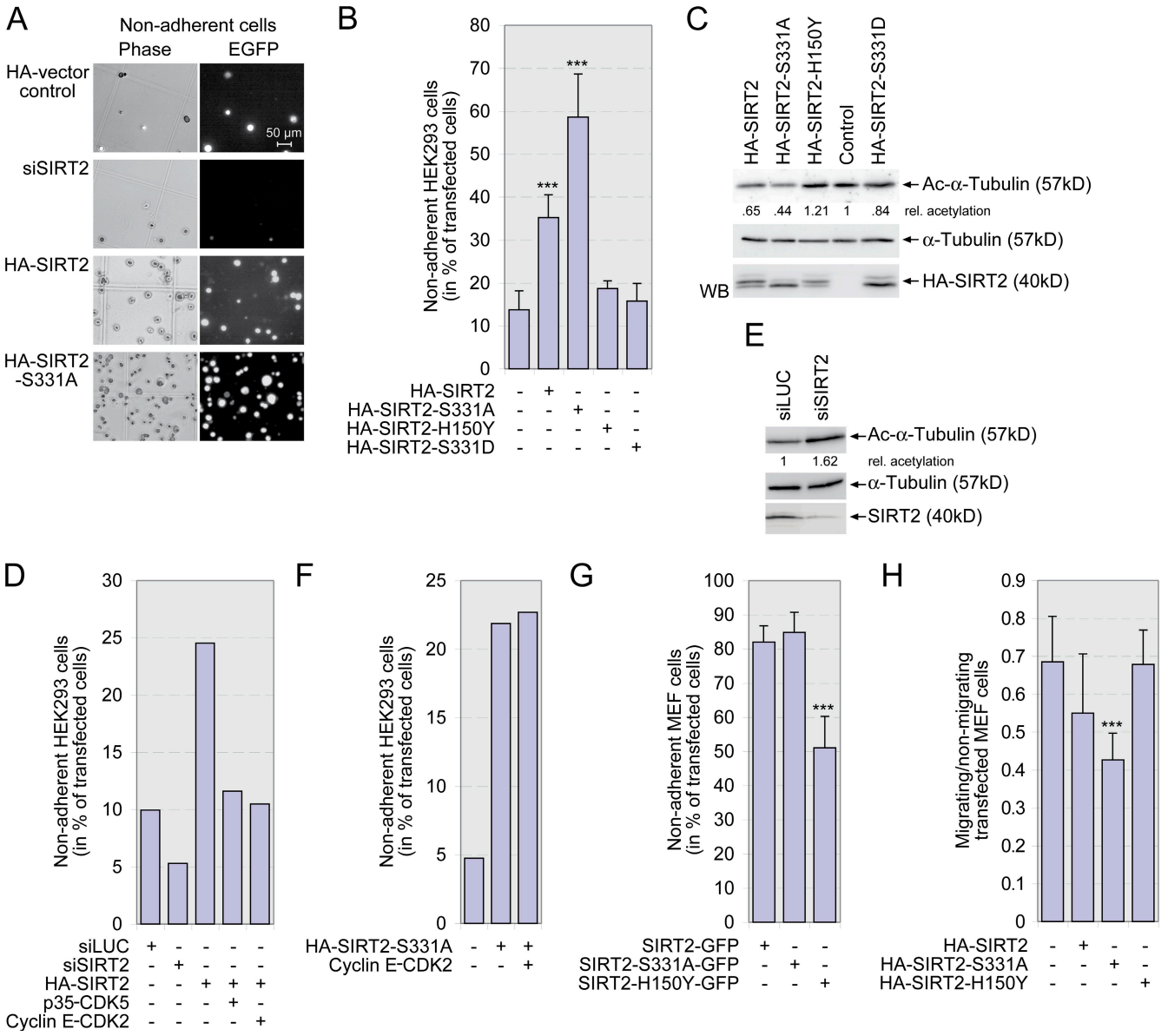

Figure 4. **SIRT2 affects cell attachment and mobility.** (A) HEK293 cells were transiently transfected with plasmids encoding 0.5 µg EGFP–α-tubulin, 20 µg HA-SIRT2, or 20 µg HA-SIRT2-S331A and 20 µg of a siRNA-expressing plasmid (siSIRT2). The cells from equal aliquots of the culture supernatants were analyzed by phase contrast and fluorescence microscopy. (B) The percentage of transfected cells (EGFP positive) of the adherent and the detached cell population was determined as in A. Displayed is the percentage of transfected cells that were detached. Mean values and SD of three experiments are shown. (C) HEK293 cells were transfected with plasmids expressing the indicated SIRT2 proteins and a plasmid coding for CD4. Transfected cells were selected using magnetic beads coated with CD4-specific antibodies. Equal amounts of cell lysates were analyzed by Western blotting for α-tubulin acetylation. (D) HEK293 cells were transiently transfected as in A, but with the following amounts of plasmids: 20 µg siSIRT2, 20 µg siLUC, 10 µg HA-SIRT2, 5 µg Cdk5, 0.5 µg cyclin E, 0.5 µg Cdk2, and 0.5 µg EGFP–α-tubulin. The analysis was performed as described in B. Mean values of two experiments are shown. (E) HEK293 cells were transiently transfected with plasmids expressing siSIRT2, siLUC, and CD4. α-Tubulin acetylation was analyzed in lysates of CD4-positive cells. The levels of SIRT2 were determined after immunoprecipitation (polyclonal serum 749) and Western blot analysis (mAb 7G5). (F) The experiment was performed as described in D. Mean values of two experiments are shown. (G) MEFs were transfected with plasmids expressing the indicated SIRT2-GFP fusion proteins. Trypsinized cells were replated on laminin-coated coverslips for 30 min. Nonadherent and adherent cells were counted. Mean values and SD of three independent experiments are displayed. (H) MEFs were transfected with the indicated expression plasmids. Confluent cell layers were scratched and the ratio of migrating versus nonmigrating transfected cells was determined. Mean values and SD of three to five experiments are shown. *, P < 0.05; **, P < 0.01; ***, P < 0.001.

Importantly, the effect of SIRT2, but not of SIRT2-S331A, was reverted by p35–Cdk5 (Fig. 6 D). Because SIRT2 and SIRT2-S331A stabilized growth cones upon ephrin-A5 treatment, we investigated the effect of SIRT2 KD on growth cones, expecting that reduced SIRT2 expression would sensitize these structures to ephrin-A5-Fc treatment. However, already in the absence of ephrin-A5-Fc a strong effect on growth cones was observed (Fig. 6 E). Growth cones of siSIRT2-treated neurons protruded significantly less filopodia in comparison to siLUC control–treated cells. Thus, in cells in which SIRT2 was knocked down, a collapsed morphology was observed already in the absence of ephrin-A5-Fc. In support of this, the KD of SIRT2 also resulted

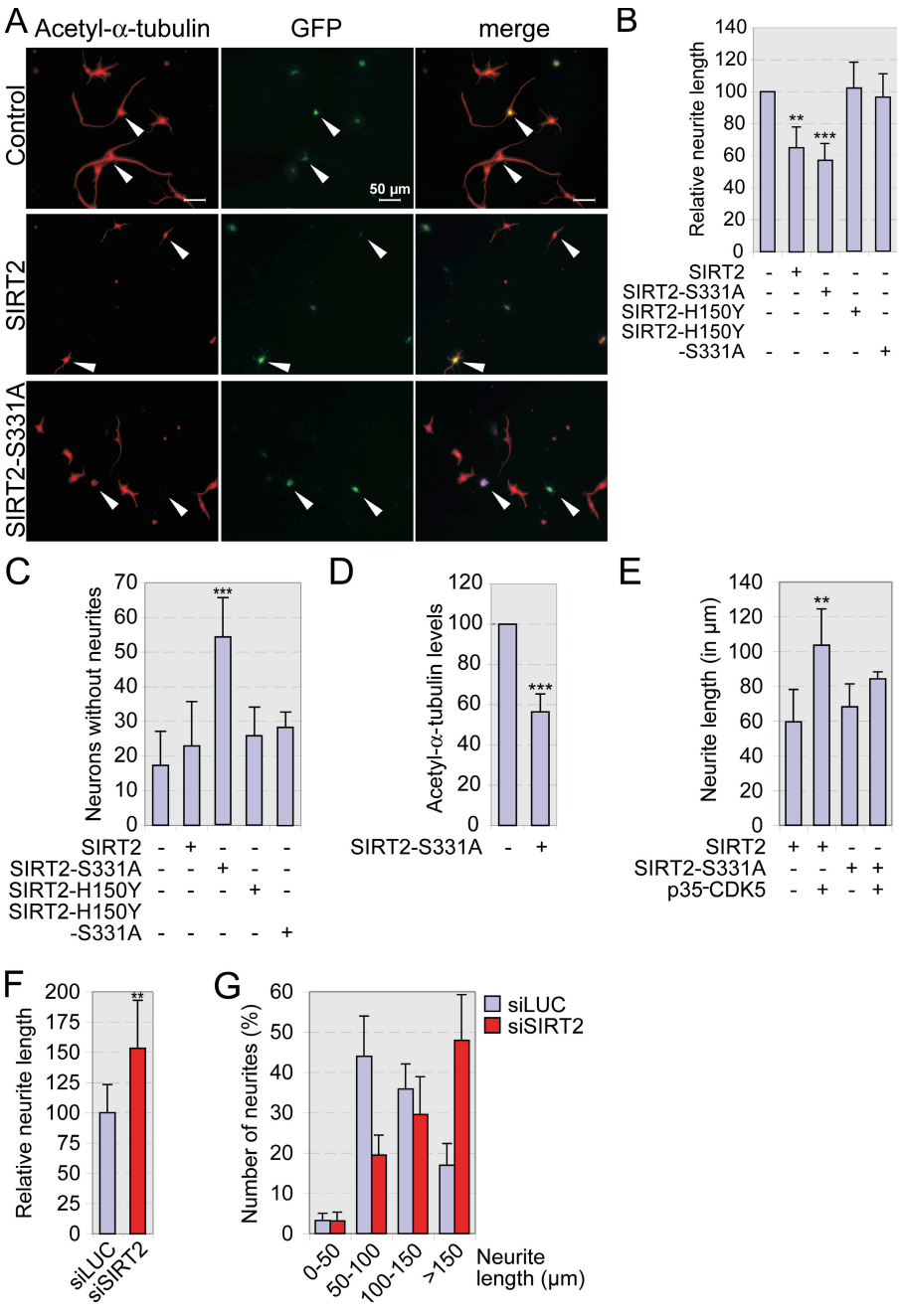

Figure 5. **SIRT2 modulates neurite outgrowth of hippocampal neurons.** (A) Hippocampal neurons were coelectroporated with constructs expressing the indicated SIRT2 proteins and a GFP vector and cultivated for 2 d in vitro, followed by staining for acetylated α-tubulin. Arrowheads identify some of the GFP-expressing cells. Bars, 50 μm. (B) Quantification of experiments exemplified in A. The neurite length was determined in response to the expressed proteins indicated. The neurite length of neurons electroporated with the parental vector was set to 100%. Only neurons with measurable neurites were taken into account. Relative neurite length is expressed in percentage of control (set to 100%). (C) Neurons without any detectable neurite growth were determined in response to the indicated SIRT2 proteins. (D) The level of acetyl-α-tubulin in SIRT2-S331A–expressing and control electroporated neurons was compared. A total of 60 neurons (20 in each of three independent experiments) were captured and acetylated α-tubulin levels measured using AxioVision software. The values from control cells were set to 100%. (E) Neurite length was measured, as in A, in response to coexpressed p35–Cdk5. (F) Neurons were coelectroporated with vectors expressing GFP and the indicated siRNAs. The neurite length of neurons electroporated with siLUC was set to 100%. Relative neurite length is expressed in percentage of control (set to 100%). (G) The neurites were classified into four length groups, from very short (0–50 μm) to very long (>150 μm). The percentage of neurons within each group is displayed. Error bars represent SD. **, $P < 0.01$; ***, $P < 0.001$.

in an ∼25% reduction in F-actin content in growth cones in the absence of ephrin-A5 ($n = 100$ growth cones each; unpublished data), which is consistent with morphological alterations observed in these growth cones (Fig. 6 E). In summary, these findings suggest strongly that the EphA-stimulated growth cone collapse is mediated at least in part by the phosphorylation and thereby repression of the deacetylase activity of SIRT2.

Discussion

Sirtuins have received considerable attention because of their role in aging, neuroprotection, and gene transcription (Haigis and Guarente, 2006; Michan and Sinclair, 2007). We identified SIRT2 in a phosphorylation screen with recombinant cyclin E–Cdk2. Cdks phosphorylate Ser-331 within a Cdk consensus sequence of SIRT2 that is conserved in several Sirtuin family members (Figs. 1, 2, and S2). Mechanistically, phosphorylation at this site represses the enzymatic activity of SIRT2 (Fig. 3), representing the first account of a posttranslational modification linked to SIRT2 enzymatic activity. Recently, the comparable site in an alternatively spliced version of SIRT2 was identified as cyclin B–Cdk1 substrate but no function was assigned to this modification (North and Verdin, 2007b). This may be because of the relative low activity of cyclin B–Cdk1 toward SIRT2 in comparision to the Cdk2 complexes as observed both in vitro and in cells (Figs. 1 and 2).

To date, two SIRT2 substrates, α-tubulin and histone H4, have been described (Dryden et al., 2003; North et al., 2003;

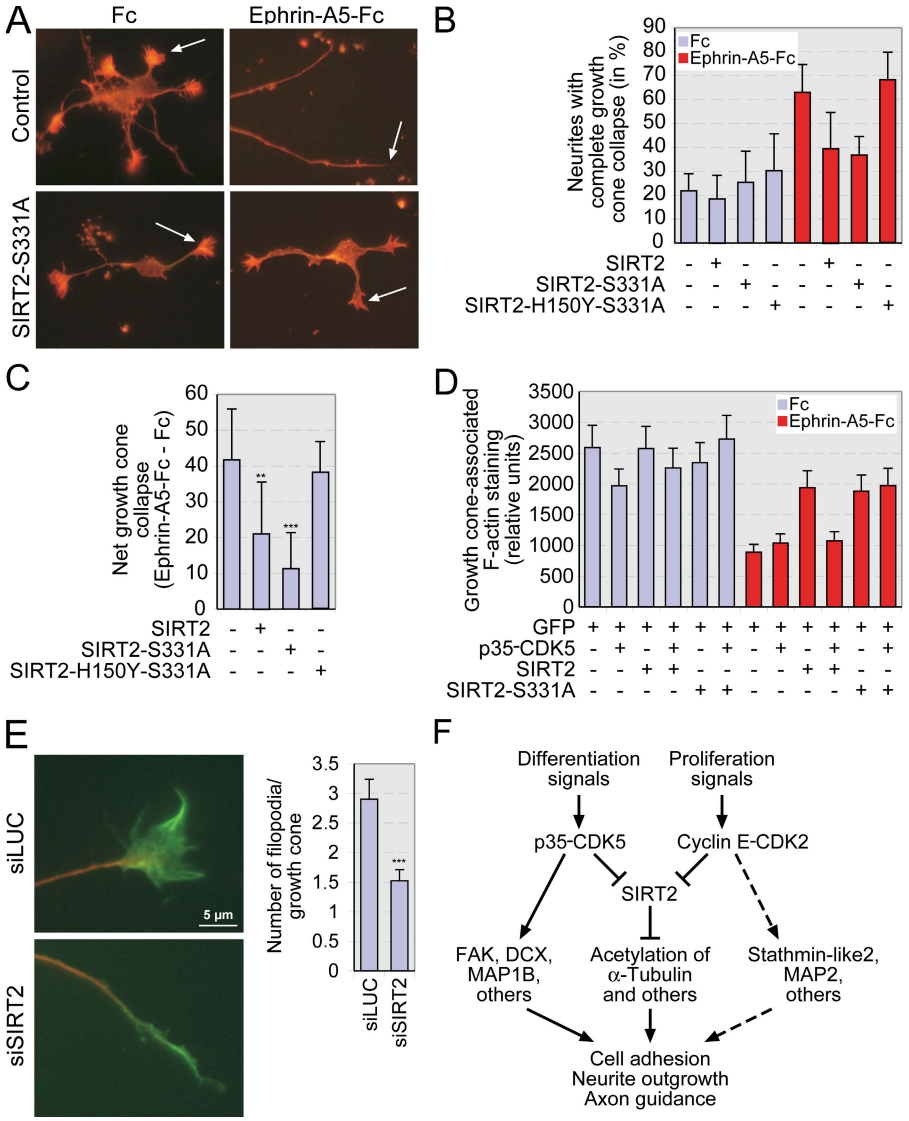

Figure 6. **SIRT2 overexpression impairs ephrin-A–mediated growth cone collapse.** (A) Hippocampal neurons were coelectroporated with constructs expressing the indicated SIRT2 proteins and a GFP vector. The cells were cultivated on laminin for 2 d and then treated with 1 µg/ml ephrin-A5-Fc or Fc for 30 min and subsequently stained for F-actin. (B) The percentage of collapsed growth cones was quantified by morphological criteria. (C) Summary of the overall change in the growth cone collapse rate. The percentage of growth cone collapse in response to ephrin-A5-Fc was subtracted from the response to Fc alone. (D) Neurons were coelectroporated with constructs expressing the indicated proteins. The cells were then stained for F-actin and the fluorescence intensity of individual growth cones was determined. Untreated growth cones contain high F-actin levels, which are decreased upon ephrin-A5 treatment. The mean values and SD of 50 or more individual growth cones/conditions are displayed. (E) Neurons were coelectroporated with constructs expressing siSIRT2 or siLUC. Growth cones were stained for β-tubulin (left, red) and F-actin (left, green). Quantification of the mean number of filopodia/growth cones after siSIRT2 or siLUC treatment is shown on the right. (F) Model of SIRT2 function and regulation by Cdk complexes. For details, see Discussion. Error bars represent SD. **, $P < 0.01$; ***, $P < 0.001$.

Vaquero et al., 2006). SIRT2 deacetylates histone H4 at Lys-16 during G_2/M, during which a subfraction of SIRT2 associates with chromatin. Deacetylation of H4K16 was suggested to be relevant for efficient chromatin condensation (Vaquero et al., 2006). The lack of SIRT2 results in a decrease in S-phase and increase in G_1-phase in MEFs without apparent effect on mitosis. In contrast, in human tumor cells overexpression of SIRT2 delayed exit from mitosis, probably because of altered α-tubulin acetylation (Dryden et al., 2003). Recently, SIRT2 was shown to inhibit mitotic slippage in cells treated with mitotic spindle drugs (Inoue et al., 2007; North and Verdin, 2007b), suggesting a role in genetic stability. In agreement with this, SIRT2 is downregulated in certain tumors (Hiratsuka et al., 2003; Matsushita et al., 2005; Voelter-Mahlknecht et al., 2005; Inoue et al., 2007). Our own analysis did not reveal any reproducible effects on mitosis in response to SIRT2, SIRT2 mutants, or KD of SIRT2 in tumor cell lines in the absence of stress (Fig. S4).

We provide evidence that SIRT2 impairs cell motility, at least in part by influencing microtubule dynamics, which is a function regulated by Cdk phosphorylation. α-Tubulin acetylation is associated with stable microtubules (Dent and Gertler, 2003; Westermann and Weber, 2003). We used multiple assays to investigate a role for SIRT2 in cell motility, including adhesion, migration, neurite outgrowth, and growth cone collapse (Figs. 4–6). All the aforementioned processes share signaling through focal contacts leading to attachment/detachment of cells from their substratum. Because microtubules and focal adhesions show extensive crosstalk (Ezratty et al., 2005), it is possible that α-tubulin deacetylation also affects the activities of focal adhesions. An increase in microtubule dynamics because of a reduction in α-tubulin acetylation might modulate focal adhesion turnover and thereby control cell motility. In neurons, an important cross talk between dynamic microtubules and actin filaments takes place at the central/peripheral growth cone interface to regulate target-directed advancement of the growth cone (Dent and Gertler, 2003). Microtubules have been shown to be crucially involved in both neurite outgrowth and chemotactic sensing of guidance cues in the surrounding of navigating growth cones (Gordon-Weeks, 2004). In neurons, acetylated microtubules are polarized toward the starting point

of the first nerve fiber protrusion (de Anda et al., 2005). It is possible that deacetylation of α-tubulin might block directed protrusion of a neurite, which would be consistent with our observation that SIRT2 inhibits neurite outgrowth (Fig. 5). The most dramatic effects were observed with nonphosphorylatable SIRT2-S331A.

Cdk5 is essential for neurite outgrowth during neuronal differentiation (Nikolic et al., 1996) and is required, together with its regulatory subunits, for the cytoarchitecture of the central nervous system (Dhavan and Tsai, 2001). Cdk5 has been implicated in the regulation of the actin and microtubule network by phosphorylating several proteins associated with these cytoskeletal components, including $p27^{KIP1}$, PAK1, FAK, doublecortin, and microtubule-associated proteins (MAPs) like MAP1B and tau (Nikolic et al., 1998; Xie et al., 2003; Drewes, 2004; Tanaka et al., 2004; Kawauchi et al., 2006). Of interest is the analysis of $p27^{KIP1}$, which is a substrate of both Cdk2 and 5. However, different sites are phosphorylated. Cdk2 modifies Thr-187, stimulating degradation, and Cdk5 phosphorylates Ser-10, enhancing stability in a cell type–specific manner. The latter is observed in neurons and is necessary for neuronal migration (Kawauchi et al., 2006). In other situations, the precise function of Cdk5-dependent phosphorylation may be less well understood; however, in general, stabilization of microtubules is observed. It is noteworthy that Cdk5 was previously shown to be an important downstream effector of the EphA receptor (Cheng et al., 2003; Fu et al., 2007). Hence, the EphA-Cdk5-SIRT2 signaling cascade might ensure full growth cone collapse. In this respect, Cdk phosphorylation and thereby inactivation of SIRT2-mediated α-tubulin deacetylation might contribute toward maintaining stable microtubules. Besides α-tubulin, we cannot rule out additional SIRT2 substrates that might contribute to the cell motility phenotypes reported here. Indeed, the recent identification of several cytoplasmic proteins, which are acetylated (Kim et al., 2006), suggests that SIRT2 and other cytoplasmic deacetylases will have additional substrates that will be important to define in the future.

Cyclin E–Cdk2 is implicated in the development of human tumors (Musgrove, 2006). The identification of SIRT2 as a novel substrate and its role in cell motility suggests that cyclin E–Cdk2 can regulate distinct aspects of the cytoskeleton. This raises the question of how these kinases get access to cytoskeletal components because both cyclin E–Cdk2 and cyclin A–Cdk2 are predominantly nuclear. A recent study demonstrates that both kinase complexes shuttle between the nuclear and cytoplasmic compartments, enabling access to cytoplasmic substrates (Jackman et al., 2002). In addition to its interaction with SIRT2 (Fig. 2), a role of Cdk2 in microtubule dynamics is supported by the identification of stathmin-like 2 (STMN2 or SCG10; Grenningloh et al., 2004; Morii et al., 2006) and MAP2 (Dehmelt and Halpain, 2004) as potential substrates (Table I). STMN2 and MAP2 influence microtubule stability, are regulated by Cdk5, and affect neurite outgrowth (Dent and Gertler, 2003). Collectively, these findings suggest that cyclin E–Cdk2, activated by proliferation signals or oncogenic mutations, regulates microtubule dynamics by phosphorylating several substrates associated with microtubules (Fig. 6 F). This could be relevant for different aspects of tumor cell biology, including elevated cell migration and cell cycle progression.

Materials and methods

Cells, transfections, and assays

HEK293, MEF, and HeLa cells were cultured in DME supplemented with penicillin/streptomycin and 10% FCS. Transient transfection assays were performed as described previously (Luscher-Firzlaff et al., 2006). HEK293 Flp-In T-REx 293 cells (Invitrogen) were stably transfected with pcDNA5/FRT/TO/N-TAP-SIRT2 or -SIRT2-S331A by coexpressing the Flp recombinase. Cell lysates of HDFs were obtained from J. Baron and U. Linzen (Rheinisch-Westfälische Technische Hochschule Aachen University, Aachen, Germany). Preparation and electroporation of primary hippocampal cultures were performed as described previously (Knoll et al., 2006). In brief, hippocampi of P1-P3 mice were incubated in trypsin-EDTA at 37°C for 10 min, followed by washing in HBSS and resuspending in prewarmed DME/10% horse serum (HS). The tissue was triturated using flame-polished Pasteur pipettes and spun down for 5 min at 600 rpm and the pellet was reconstituted in DME/HS. After counting, the cells were pelleted and then resuspended in mouse neuron Nucleofector solution (Amaxa) as recommended by the manufacturer. A total of 3 µg DNA (2.25 µg of the desired construct and 0.75 µg of permuted EGFP) was used for electroporation per sample. Cultures were plated in neurobasal medium supplemented with B27 supplement (Invitrogen) for 2 d in vitro. The significance of experimental results was determined by *t* test (two sided), with one asterisk indicating $P < 0.05$, two asterisks $P < 0.01$, and three asterisks $P < 0.001$.

To determine the detached cells, transiently transfected HEK293 cells were identified by analyzing EGFP-positive cells. 2 d after transfection, the number of transfected detached and transfected adherent cells was counted, and from this the rate of detachment was determined.

For cell migration, 10^5 MEFs were plated in one well of a 24-well plate, followed by transfection with Lipofectamine for 6–8 h in Optimem (0.6 µg SIRT2 construct plus 0.2 µg GFP/well). The next day, a scratch was applied and cell migration into the cleared area was monitored 12 and 24 h afterward. The number of GFP-positive cells in and outside the scratch was determined along with bright field recording.

To determine the effect of SIRT2 on α-tubulin acetylation in cells, HEK293 cells were cotransfected with plasmids expressing SIRT2 and the human CD4 antigen with a truncated cytoplasmic domain (pMACS4.1; Miltenyi Biotec) at a ratio of 3:1. CD4-positive cells were selected using magnetic beads coated with antibody specific for CD4 according to the manufacturer's instruction (Dynabeads CD4; Invitrogen). Selected cells were lysed in RIPA buffer (10 mM Tris-HCl, pH 7.4, 150 mM NaCl, 1% NP-40, 1% deoxycholate, 0.1% SDS, 7 µg/ml aprotinin, and 20 mM β-glycerophosphate), and α-tubulin, acetylated α-tubulin, and SIRT2 were detected by immunoblotting.

Plasmid constructs

All SIRT2 constructs and Cdk5 were generated by recombining the PCR-amplified ORF into pDonR201 of the Gateway cloning system (Invitrogen) by virtue of attB1 and attB2-mediated BP-clonase reaction. A subsequent LR-recombination reaction with Gateway-compatible pGex4T2 and pEVRF0-HA resulted in GST- and HA-tagged expression constructs. Site-directed mutagenesis was performed using the quick change protocol (Stratagene) to generate the S331A, S331D, S331E, H150Y, and S331A-H150Y mutants. All constructs were verified by DNA sequencing. pCMV-EGFP-tubulin was cloned by standard procedures. For constructs expressing siRNA specific for SIRT2, the sequence 5′-GATCCCCGTT CACAGCCTAG AATATATTCA AGAGATATAT TCTAGGCTGT GAACTTTTTG GAAA-3′was cloned into pSUPER (provided by R. Bernards, Netherlands Cancer Institute, Amsterdam, Netherlands). This sequence is identical for both human and mouse. For a mouse-specific siSIRT2, the sequence 5′-GATCCCCCTT CCACCGCGCT TCTTCTTTCA AGAGAAGAAG AAGCGCGGTG GAAG-TTTTTG GAAA-3′ was used. Additional constructs have been described previously (Rottmann et al., 2005; Luscher-Firzlaff et al., 2006).

Preparation of active cyclin–Cdk complexes

Expression and purification of human cyclin D, A, and E in complexes with Cdk2 and 4 from insect cells coinfected with recombinant baculoviruses were performed as previously described (Sarcevic et al., 1997). Baculoviruses expressing cyclin B and Cdk1 were provided by D. Morgan (University of California, San Francisco, San Francisco, CA). The activities of Cdk4 or Cdk2 and 1 complexes were measured using $pRb^{778\text{-}928}$ or histone

H1, respectively. 1 catal of cyclin–Cdk activity incorporates 1 mol/s of phosphate in 30 µl of kinase buffer (50 mM Hepes, pH 7.5, 10 mM $MgCl_2$, 0.01% Tween-20, 10 mM NaF, 10 mM β-glycerophosphate, 1 mM orthovanadate, 0.01% BSA, and 25 µM ATP) containing 5 µg $pRb^{778\text{-}928}$ or histone H1 and 25 µM ATP. The incorporation of phosphate was linear over the incubation time of 30 min. The p35–Cdk5 complex was obtained from Millipore.

Solid phase phosphorylation

High-density protein arrays enriched for high expression of His_6-tagged proteins were obtained from the German Resource Center for Genome Research (hEx1 library; http://www.rzpd.de). For phosphorylation cloning, filters were rehydrated and the cell debris was washed off twice in 20 mM Tris-Cl, pH 7.5, 0.5 M NaCl, and 0.5% Tween-20 for 10 min each. Further processing steps were three incubations in 20 mM Tris-Cl, pH 7.5, 0.5 M NaCl, 20 mM Tris-Cl, pH 7.5, 0.5% Tween-20, 10 mM EDTA, 1 mM EGTA, 1 mM DTT, 0.2 mM PMSF, and 3% BSA for 10 min each. Filters were briefly equilibrated in kinase buffer and then incubated in the same buffer at room temperature for 1 h. Next, the filters were subjected to phosphorylation by incubation in kinase buffer supplemented with 2.5 pcatal/ml cyclin E–Cdk2 and 200 kBq/ml γ-[^{32}P]ATP at 30°C for 90 min. Finally, filters were washed in 50 mM Hepes, pH 7.5, 10 mM $MgCl_2$, 250 mM NaCl, and 0.2 mM PMSF and exposed to x-ray film for autoradiography.

In vitro kinase assays, in vivo labeling, and phosphatase assays

In vitro phosphorylation of purified GST fusion proteins was performed as described previously (Sarcevic et al., 1997), except that incubations were at 30°C for 30 min. For in vivo labeling, HEK293 cells were transiently transfected and, 2 d later, metabolically labeled in phosphate-free DME supplemented with 10% dialyzed FCS, 20 mM sodium bicarbonate, 18 mM Hepes, pH 7.5, and 10–20 MBq of [^{32}P]orthophosphate for 2 h. The labeled cells were lysed in RIPA buffer. The HA-tagged SIRT2 proteins were immunoprecipitated with α-HA mAb (3F10) and protein G–Agarose. The precipitates were washed four times in the same buffer and separated by SDS-PAGE on 12% gels (Luscher-Firzlaff et al., 2006).

For phosphatase treatment, cells were lysed in RIPA buffer and SIRT2 was immunoprecipitated using polyclonal antisera and washed. Immobilized proteins were resuspended in 50 mM Tris-HCl, pH 8.5, and 1 mM $MgCl_2$. The probes were then incubated in the presence of 0.7 U of bacterial alkaline phosphatase (Sigma-Aldrich) at 30°C for 30 min. The reactions were stopped by adding SDS sample buffer.

Phosphopeptide identification by nanoliquid chromatography tandem mass spectrometry

Proteins were treated with DTT and iodoacetamide and digested in gel by trypsin. Before nanoliquid chromatography tandem mass spectrometry analysis, all trypsin-digested samples were purified and desalted using C_{18} STAGE tips (Rappsilber et al., 2003).

Peptide identification experiments were performed using a nano-HPLC 1100 nanoflow system (Agilent Technologies) connected online to a 7-Tesla linear quadrupole ion trap–Fourier transform mass spectrometer (Thermo Fisher Scientific). Peptides were separated on 15 cm of 100 µm ID PicoTip columns (New Objective, Inc.) packed with 3 µm Reprosil C18 beads (Dr. Maisch, GmbH) using a 90-min gradient from 90% buffer A/10% buffer B to 65% buffer A/35% buffer B (buffer A contains 0.5% acetic acid and buffer B contains 80% acetonitrile in 0.5% acetic acid) with a flow rate of 300 nl/min. Peptides eluting from the column tip were electrosprayed directly into the mass spectrometer with a spray voltage of 2.1 kV. The mass spectrometer was operated in the data-dependent mode to sequence the four most intense ions per duty cycle. In brief, full-scan mass spectrometry spectra of intact peptides (m/z 350–2,000) with an automated gain control accumulation target value of 10^6 ions were acquired in the Fourier transform ion cyclotron resonance cell with a resolution of 50,000. The four most abundant ions were sequentially isolated and fragmented in the linear ion trap by applying collision-induced dissociation using an accumulation target value of 20,000 (capillary temperature, 200°C; normalized collision energy, 30%). A dynamic exclusion of ions previously sequenced within 180 s was applied. All unassigned charge states were excluded from sequencing. A minimum of 500 counts was required for mass spectrometry 2 selection. Data-dependent neutral loss scanning of phosphoric acid groups was enabled for each mass spectrometry 2 spectrum among the three most intense fragment ions.

RAW spectrum files were converted into a Mascot generic peak list by DTASupercharge (http://msquant.sourceforge.net). Peptides and proteins were identified using the Mascot algorithm (Matrix Science) to search a local version of the UNIprot database (release 48.0). The following initial search criteria were applied: 20 parts per million (ppm) for the parental peptide and 0.5 D for fragmentation spectra and a fixed carbamidomethyl modification for cysteines. Oxidation of methionine, deamidation (glutamine and asparagine), and phosphorylation (serine, threonine, and tyrosine) were searched as variable modifications. Parent ion masses were internally calibrated by MSQuant (http://msquant.sourceforge.net) to obtain accurate masses better than 5 ppm. Fragmentation spectra of phosphopeptides were manually verified.

Antibodies, immunoprecipitation, and Western blotting

The polyclonal anti-SIRT2 T749 and T809 antisera were raised against a bacterially expressed GST-SIRT2 fusion protein (Eurogentec). The following antibodies are commercially available from the indicated sources: Cdk2 pAb H-298, Cdk5 pAb C-8, cyclin E pAb M-20, GFP pAb (FL), p27 pAb C-19, p35 pAb C-19, and SIRT2 mAb A-5 (Santa Cruz Biotechnology, Inc.); HA-tag mAb 3F10 (Roche); and acetyl-α-tubulin mAb 6–11-B-1 and α-tubulin mAb B-5-1-2 (Sigma Aldrich). Low stringency immunoprecipitations and coimmunoprecipitations and Western blotting were done as described previously (Vervoorts et al., 2003). mAbs specific for Ser-331 phosphorylated human SIRT2 were generated against the synthetic peptide NPSTSAS(phosphorylated)PKKSPPPAKDEARTTEREKPQ in Lou/C rats.

HDAC assay

Immunoprecipitated material was washed in SIRT2 deacetylase buffer (50 mM Hepes, pH 7.5, 10 mM $MgCl_2$, 10 mM NaF, 10 mM β-glycerophosphate, 0.2 mM DTT, and 25 µM ATP), which is identical to the kinase buffer. Both immunoprecipitated material and recombinant SIRT2 were resuspended in 50 µl SIRT2 deacetylase buffer containing 1 mM NAD^+ (Sigma-Aldrich) and ^{3}H-acetylated chicken reticulocyte core histone (~7.5 µg corresponding to 12,000 cpm per reaction; obtained from P. Loidl, Innsbruck Medical University, Innsbruck, Austria). The reactions were performed in the presence of 20 µM trichostatin A to block potentially copurified HDAC activities at 37°C for 60 min. The acetyl-group of *O*-acetyl-ADP-ribose was hydrolysed by adding 15 µl of 1 N NaOH at room temperature for 20 min, followed by adding 185 µl of 0.1 M HCl and 0.16 M acetic acid. Released [^{3}H]acetate was extracted in 750 µl ethyl acetate and counted (Borra et al., 2004). Deacetylation of brain-derived α-tubulin was performed with 25 µg of P3-P4 mouse forebrain lysate essentially as described previously (North et al., 2003).

Immunocytochemistry

Cultures were fixed with PBS containing 4% paraformaldehyde and 5% sucrose for 15 min followed by washing and permeabilization in PBS with 0.1% Triton X-100 for 5 min. The samples were blocked in PBS with 2% BSA and incubated with primary antibodies for 1 h. Primary antibodies were used as follows: rabbit anti-SIRT2 (1:500), mouse anti-SIRT2 (1:50; Santa Cruz Biotechnology, Inc.), rabbit anti-p35 (1:50; Santa Cruz Biotechnology, Inc.), mouse anti–β-tubulin (1:1,500; Sigma-Aldrich), and mouse anti–acetylated α-tubulin (1:1,500). Secondary antibodies conjugated to Alexa488, 546, or 660 (1:1,000; Invitrogen) were applied for 1 h along with Texas red phalloidin (Invitrogen) to highlight filamentous actin. After washing with PBS and staining with DAPI for 5 min, coverslips were mounted with mowiol. Images of cells were acquired at room temperature on a microscope (Axiovert; Carl Zeiss, Inc.) using either a 20× Plan-Neofluar 0.5 NA (Carl Zeiss, Inc.) or a 63× Plan-Neofluar 1.3 NA (Carl Zeiss, Inc.) lens without oil. A camera (AxioCam; Carl, Zeiss Inc.) with AxioVision 4.6 software (Carl Zeiss, Inc.) for deconvolution and Photoshop CS (Adobe) for adjusting contrast and brightness was used.

Colocalization of SIRT2 and p35 expression was performed by analyzing z stacks using AxioVision 4.6 software. Fig. S5 D is a typical result obtained from one individual section of the z-stack series. Fields 1 and 2 contain pixels of SIRT2 and p35, respectively, not colocalizing, whereas area 3 reveals pixels overlapping (area 4 contains largely background signals surrounding the cells; Fig. S5 D).

Neurite outgrowth and growth cone collapse assays

Acid-treated coverslips (diameter, 13 mm) were coated with 100 µg/ml poly-L-lysine (Sigma-Aldrich) in borate buffer at 37°C for 1 h, followed by washing and incubating with 20 µg/ml mouse laminin (Invitrogen) in HBSS at 37°C for 3–4 h. After additional washing steps, coverslips were kept in DME with 10% HS at 37°C until used. Neurons were plated at a density of $5 \times 10^3 - 2 \times 10^4$ cells per coverslip and stained after 2 d of in vitro culture. For growth cone collapse assays, 2-d-old cultures were incubated at 37°C for 30 min with 1 µg/ml of preclustered ephrin-A5-Fc with 10 µg/ml anti–human IgG, Fc-specific, for 30 min (Sigma-Aldrich) or Fc alone followed by staining for F-actin and microtubules.

For neurite outgrowth assays, the maximal achievable neurite length per neuron of more than 40 neurons per mouse was measured using Axiovision software. In the growth cone collapse assay, all growth cones (~2–5) of a given neuron using a total of >50 neurons per mouse were scored. Only growth cones without any remaining filopodia were scored as fully collapsed.

Online supplemental material

Fig. S1 shows the differential substrate specificity of distinct cyclin-dependent kinase complexes. Fig. S2 displays that SIRT2 is phosphorylated by cyclin A–Cdk2 but not by D-type cyclin complexes. Fig. S3 shows the expression pattern of deacetylases in the hippocampus of 2-wk-old mice. Fig. S4 demonstrates that SIRT2 overexpression does not affect cell proliferation. Fig. S5 reveals colocalization of SIRT2 and p35 in mouse primary hippocampal neurons. Online supplemental material is available at http://www.jcb.org/cgi/content/full/jcb.200707126/DC1.

We wish to thank R. Bernards and P. Loidl for reagents, J. Baron for primary HDFs, U. Linzen for whole cell extracts of serum-stimulated primary HDFs, and E. Barczak, E. Buerova, B. Habermehl, D. Sinske, and J. Stahl for excellent technical assistance. We also thank J. Weis and C. Weinl for critical reading of the manuscript.

This work was supported by a PhD stipend of the Rheinisch-Westfälische Technische Hochschule to R. Pandithage, the Emmy-Noether program of the Deutsche Forschungsgemeinschaft, the SFB446 of the Deutsche Forschungsgemeinschaft, the Schram-Stiftung, a young investigator award of the University of Tübingen to B. Knöll, and a START grant and the Bonus Program of the Medical School of the Rheinisch-Westfälische Technische Hochschule to R. Lilischkis and B. Lüscher. The authors declare no financial competing interests.

Submitted: 18 July 2007
Accepted: 6 February 2008

References

Amati, B., K. Alevizopoulos, and J. Vlach. 1998. Myc and the cell cycle. *Front. Biosci.* 3:d250–d268.

Borra, M.T., M.R. Langer, J.T. Slama, and J.M. Denu. 2004. Substrate specificity and kinetic mechanism of the Sir2 family of NAD+-dependent histone/protein deacetylases. *Biochemistry.* 43:9877–9887.

Bussow, K., D. Cahill, W. Nietfeld, D. Bancroft, E. Scherzinger, H. Lehrach, and G. Walter. 1998. A method for global protein expression and antibody screening on high-density filters of an arrayed cDNA library. *Nucleic Acids Res.* 26:5007–5008.

Cheng, Q., Y. Sasaki, M. Shoji, Y. Sugiyama, H. Tanaka, T. Nakayama, N. Mizuki, F. Nakamura, K. Takei, and Y. Goshima. 2003. Cdk5/p35 and Rho-kinase mediate ephrin-A5-induced signaling in retinal ganglion cells. *Mol. Cell. Neurosci.* 24:632–645.

de Anda, F.C., G. Pollarolo, J.S. Da Silva, P.G. Camoletto, F. Feiguin, and C.G. Dotti. 2005. Centrosome localization determines neuronal polarity. *Nature.* 436:704–708.

Dehmelt, L., and S. Halpain. 2004. Actin and microtubules in neurite initiation: are MAPs the missing link? *J. Neurobiol.* 58:18–33.

Dent, E.W., and F.B. Gertler. 2003. Cytoskeletal dynamics and transport in growth cone motility and axon guidance. *Neuron.* 40:209–227.

Dhavan, R., and L.H. Tsai. 2001. A decade of Cdk5. *Nat. Rev. Mol. Cell Biol.* 2:749–759.

Drewes, G. 2004. MARKing tau for tangles and toxicity. *Trends Biochem. Sci.* 29:548–555.

Dryden, S.C., F.A. Nahhas, J.E. Nowak, A.S. Goustin, and M.A. Tainsky. 2003. Role for human SIRT2 NAD-dependent deacetylase activity in control of mitotic exit in the cell cycle. *Mol. Cell. Biol.* 23:3173–3185.

Ezratty, E.J., M.A. Partridge, and G.G. Gundersen. 2005. Microtubule-induced focal adhesion disassembly is mediated by dynamin and focal adhesion kinase. *Nat. Cell Biol.* 7:581–590.

Freeman, R.S., S. Estus, and E.M. Johnson Jr. 1994. Analysis of cell cycle-related gene expression in postmitotic neurons: selective induction of cyclin D1 during programmed cell death. *Neuron.* 12:343–355.

Frye, R.A. 1999. Characterization of five human cDNAs with homology to the yeast SIR2 gene: Sir2-like proteins (sirtuins) metabolize NAD and may have protein ADP-ribosyltransferase activity. *Biochem. Biophys. Res. Commun.* 260:273–279.

Fu, W.Y., Y. Chen, M. Sahin, X.S. Zhao, L. Shi, J.B. Bikoff, K.O. Lai, W.H. Yung, A.K. Fu, M.E. Greenberg, and N.Y. Ip. 2007. Cdk5 regulates EphA4-mediated dendritic spine retraction through an ephexin1-dependent mechanism. *Nat. Neurosci.* 10:67–76.

Gavet, O., S. Ozon, V. Manceau, S. Lawler, P. Curmi, and A. Sobel. 1998. The stathmin phosphoprotein family: intracellular localization and effects on the microtubule network. *J. Cell Sci.* 111:3333–3346.

Gordon-Weeks, P.R. 2004. Microtubules and growth cone function. *J. Neurobiol.* 58:70–83.

Grenningloh, G., S. Soehrman, P. Bondallaz, E. Ruchti, and H. Cadas. 2004. Role of the microtubule destabilizing proteins SCG10 and stathmin in neuronal growth. *J. Neurobiol.* 58:60–69.

Haigis, M.C., and L.P. Guarente. 2006. Mammalian sirtuins–emerging roles in physiology, aging, and calorie restriction. *Genes Dev.* 20:2913–2921.

Hiratsuka, M., T. Inoue, T. Toda, N. Kimura, Y. Shirayoshi, H. Kamitani, T. Watanabe, E. Ohama, C.G. Tahimic, A. Kurimasa, and M. Oshimura. 2003. Proteomics-based identification of differentially expressed genes in human gliomas: down-regulation of SIRT2 gene. *Biochem. Biophys. Res. Commun.* 309:558–566.

Hou, Z., Q. Li, L. He, H.Y. Lim, X. Fu, N.S. Cheung, D.X. Qi, and R.Z. Qi. 2007. Microtubule association of the neuronal p35 activator of Cdk5. *J. Biol. Chem.* 282:18666–18670.

Hubbert, C., A. Guardiola, R. Shao, Y. Kawaguchi, A. Ito, A. Nixon, M. Yoshida, X.F. Wang, and T.P. Yao. 2002. HDAC6 is a microtubule-associated deacetylase. *Nature.* 417:455–458.

Inoue, T., M. Hiratsuka, M. Osaki, H. Yamada, I. Kishimoto, S. Yamaguchi, S. Nakano, M. Katoh, H. Ito, and M. Oshimura. 2007. SIRT2, a tubulin deacetylase, acts to block the entry to chromosome condensation in response to mitotic stress. *Oncogene.* 26:945–957.

Jackman, M., Y. Kubota, N. den Elzen, A. Hagting, and J. Pines. 2002. cyclin A- and cyclin E-Cdk complexes shuttle between the nucleus and the cytoplasm. *Mol. Biol. Cell.* 13:1030–1045.

Jiang, W., G. Jimenez, N.J. Wells, T.J. Hope, G.M. Wahl, T. Hunter, and R. Fukunaga. 1998. PRC1: a human mitotic spindle-associated Cdk substrate protein required for cytokinesis. *Mol. Cell.* 2:877–885.

Kawauchi, T., K. Chihama, Y. Nabeshima, and M. Hoshino. 2006. Cdk5 phosphorylates and stabilizes p27kip1 contributing to actin organization and cortical neuronal migration. *Nat. Cell Biol.* 8:17–26.

Keyomarsi, K., S.L. Tucker, and I. Bedrosian. 2003. cyclin E is a more powerful predictor of breast cancer outcome than proliferation. *Nat. Med.* 9:152.

Kim, S.C., R. Sprung, Y. Chen, Y. Xu, H. Ball, J. Pei, T. Cheng, Y. Kho, H. Xiao, L. Xiao, et al. 2006. Substrate and functional diversity of lysine acetylation revealed by a proteomics survey. *Mol. Cell.* 23:607–618.

Knoll, B., and U. Drescher. 2002. Ephrin-As as receptors in topographic projections. *Trends Neurosci.* 25:145–149.

Knoll, B., O. Kretz, C. Fiedler, S. Alberti, G. Schutz, M. Frotscher, and A. Nordheim. 2006. Serum response factor controls neuronal circuit assembly in the hippocampus. *Nat. Neurosci.* 9:195–204.

Kouzarides, T. 2000. Acetylation: a regulatory modification to rival phosphorylation? *EMBO J.* 19:1176–1179.

Li, W., B. Zhang, J. Tang, Q. Cao, Y. Wu, C. Wu, J. Guo, E.A. Ling, and F. Liang. 2007. Sirtuin 2, a mammalian homolog of yeast silent information regulator-2 longevity regulator, is an oligodendroglial protein that decelerates cell differentiation through deacetylating alpha-tubulin. *J. Neurosci.* 27:2606–2616.

Luscher, B. 2001. Function and regulation of the transcription factors of the Myc/Max/Mad network. *Gene.* 277:1–14.

Luscher-Firzlaff, J.M., R. Lilischkis, and B. Luscher. 2006. Regulation of the transcription factor FOXM1c by cyclin E/Cdk2. *FEBS Lett.* 580:1716–1722.

Malumbres, M., and M. Barbacid. 2005. Mammalian cyclin-dependent kinases. *Trends Biochem. Sci.* 30:630–641.

Marshall, R.M., and X. Grana. 2006. Mechanisms controlling Cdk9 activity. *Front. Biosci.* 11:2598–2613.

Matsushita, N., Y. Takami, M. Kimura, S. Tachiiri, M. Ishiai, T. Nakayama, and M. Takata. 2005. Role of NAD-dependent deacetylases SIRT1 and SIRT2 in radiation and cisplatin-induced cell death in vertebrate cells. *Genes Cells.* 10:321–332.

Michan, S., and D. Sinclair. 2007. Sirtuins in mammals: insights into their biological function. *Biochem. J.* 404:1–13.

Morii, H., Y. Shiraishi-Yamaguchi, and N. Mori. 2006. SCG10, a microtubule destabilizing factor, stimulates the neurite outgrowth by modulating microtubule dynamics in rat hippocampal primary cultured neurons. *J. Neurobiol.* 66:1101–1114.

Musgrove, E.A. 2006. cyclins: roles in mitogenic signaling and oncogenic transformation. *Growth Factors.* 24:13–19.

Nebreda, A.R. 2006. Cdk activation by non-cyclin proteins. *Curr. Opin. Cell Biol.* 18:192–198.

Nikolic, M. 2004. The molecular mystery of neuronal migration: FAK and Cdk5. *Trends Cell Biol.* 14:1–5.

Nikolic, M., H. Dudek, Y.T. Kwon, Y.F. Ramos, and L.H. Tsai. 1996. The cdk5/p35 kinase is essential for neurite outgrowth during neuronal differentiation. *Genes Dev.* 10:816–825.

Nikolic, M., M.M. Chou, W. Lu, B.J. Mayer, and L.H. Tsai. 1998. The p35/Cdk5 kinase is a neuron-specific Rac effector that inhibits Pak1 activity. *Nature.* 395:194–198.

North, B.J., and E. Verdin. 2007a. Interphase nucleo-cytoplasmic shuttling and localization of SIRT2 during mitosis. *PLoS ONE.* 2:e784.

North, B.J., and E. Verdin. 2007b. Mitotic regulation of SIRT2 by Cdk1-dependent phosphorylation. *J. Biol. Chem.* 282:19546–19555.

North, B.J., B.L. Marshall, M.T. Borra, J.M. Denu, and E. Verdin. 2003. The human Sir2 ortholog, SIRT2, is an NAD+-dependent tubulin deacetylase. *Mol. Cell.* 11:437–444.

Nurse, P. 2000. A long twentieth century of the cell cycle and beyond. *Cell.* 100:71–78.

Olsen, J.V., B. Blagoev, F. Gnad, B. Macek, C. Kumar, P. Mortensen, and M. Mann. 2006. Global, in vivo, and site-specific phosphorylation dynamics in signaling networks. *Cell.* 127:635–648.

Pasquale, E.B. 2005. Eph receptor signalling casts a wide net on cell behaviour. *Nat. Rev. Mol. Cell Biol.* 6:462–475.

Rappsilber, J., Y. Ishihama, and M. Mann. 2003. Stop and go extraction tips for matrix-assisted laser desorption/ionization, nanoelectrospray, and LC/MS sample pretreatment in proteomics. *Anal. Chem.* 75:663–670.

Rottmann, S., A.R. Menkel, C. Bouchard, J. Mertsching, P. Loidl, E. Kremmer, M. Eilers, J. Luscher-Firzlaff, R. Lilischkis, and B. Luscher. 2005. Mad1 function in cell proliferation and transcriptional repression is antagonized by cyclin E/Cdk2. *J. Biol. Chem.* 280:15489–15492.

Sarcevic, B., R. Lilischkis, and R.L. Sutherland. 1997. Differential phosphorylation of T-47D human breast cancer cell substrates by D1-, D3-, E-, and A-type cyclin-Cdk complexes. *J. Biol. Chem.* 272:33327–33337.

Sherr, C.J., and J.M. Roberts. 2004. Living with or without cyclins and cyclin-dependent kinases. *Genes Dev.* 18:2699–2711.

Southwood, C.M., M. Peppi, S. Dryden, M.A. Tainsky, and A. Gow. 2007. Microtubule deacetylases, SirT2 and HDAC6, in the nervous system. *Neurochem. Res.* 32:187–195.

Stachora, A.A., R.E. Schafer, M. Pohlmeier, G. Maier, and H. Ponstingl. 1997. Human Supt5h protein, a putative modulator of chromatin structure, is reversibly phosphorylated in mitosis. *FEBS Lett.* 409:74–78.

Sun, Q.Y., and H. Schatten. 2006. Role of NuMA in vertebrate cells: review of an intriguing multifunctional protein. *Front. Biosci.* 11:1137–1146.

Tanaka, T., F.F. Serneo, H.C. Tseng, A.B. Kulkarni, L.H. Tsai, and J.G. Gleeson. 2004. Cdk5 phosphorylation of doublecortin ser297 regulates its effect on neuronal migration. *Neuron.* 41:215–227.

Vaquero, A., M.B. Scher, D.H. Lee, A. Sutton, H.L. Cheng, F.W. Alt, L. Serrano, R. Sternglanz, and D. Reinberg. 2006. SirT2 is a histone deacetylase with preference for histone H4 Lys 16 during mitosis. *Genes Dev.* 20:1256–1261.

Vervoorts, J., J.M. Luscher-Firzlaff, S. Rottmann, R. Lilischkis, G. Walsemann, K. Dohmann, M. Austen, and B. Luscher. 2003. Stimulation of c-MYC transcriptional activity and acetylation by recruitment of the cofactor CBP. *EMBO Rep.* 4:484–490.

Voelter-Mahlknecht, S., A.D. Ho, and U. Mahlknecht. 2005. FISH-mapping and genomic organization of the NAD-dependent histone deacetylase gene, Sirtuin 2 (Sirt2). *Int. J. Oncol.* 27:1187–1196.

Westermann, S., and K. Weber. 2003. Post-translational modifications regulate microtubule function. *Nat. Rev. Mol. Cell Biol.* 4:938–947.

Wilson, J.M., V.Q. Le, C. Zimmerman, R. Marmorstein, and L. Pillus. 2006. Nuclear export modulates the cytoplasmic Sir2 homologue Hst2. *EMBO Rep.* 7:1247–1251.

Xie, Z., K. Sanada, B.A. Samuels, H. Shih, and L.H. Tsai. 2003. Serine 732 phosphorylation of FAK by Cdk5 is important for microtubule organization, nuclear movement, and neuronal migration. *Cell.* 114:469–482.

Xie, Z., B.A. Samuels, and L.H. Tsai. 2006. cyclin-dependent kinase 5 permits efficient cytoskeletal remodeling–a hypothesis on neuronal migration. *Cereb. Cortex.* 16:i64–i68.

Zhang, Y., N. Li, C. Caron, G. Matthias, D. Hess, S. Khochbin, and P. Matthias. 2003. HDAC-6 interacts with and deacetylates tubulin and microtubules in vivo. *EMBO J.* 22:1168–1179.

Zurita, M., and C. Merino. 2003. The transcriptional complexity of the TFIIH complex. *Trends Genet.* 19:578–584.